DESIGN OF NOVEL INHIBITORS OF TRYPANOSOMATID PARASITES

Yahan Zhang

A Thesis Submitted for the Degree of MPhil
at the
University of St Andrews

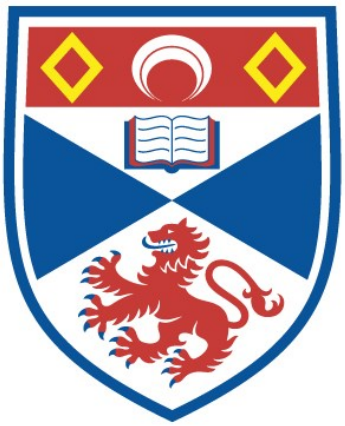

2021

Identifiers to use to cite or link to this thesis:

DOI: https://doi.org/10.17630/sta/149
http://hdl.handle.net/10023/24433

Design of Novel Inhibitors of Trypanosomatid Parasites

Yahan Zhang

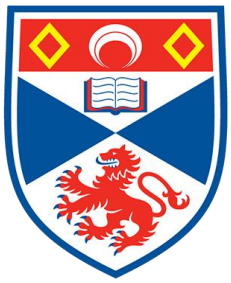

University of
St Andrews

This thesis is submitted in partial fulfilment for the degree of

Master of Philosophy (MPhil)

at the University of St Andrews

August 2021

Candidate's declaration

I, Yahan Zhang, do hereby certify that this thesis, submitted for the degree of MPhil, which is approximately 12,000 words in length, has been written by me, and that it is the record of work carried out by me, or principally by myself in collaboration with others as acknowledged, and that it has not been submitted in any previous application for any degree. I confirm that any appendices included in my thesis contain only material permitted by the 'Assessment of Postgraduate Research Students' policy.

I was admitted as a research student at the University of St Andrews in August 2019.

I, Yahan Zhang, received assistance in the writing of this thesis in respect of language, which was provided by Dr. Marija Zacharova.

I confirm that no funding was received for this work.

Date 25 August 2021 Signature of candidate

Supervisor's declaration

I hereby certify that the candidate has fulfilled the conditions of the Resolution and Regulations appropriate for the degree of MPhil in the University of St Andrews and that the candidate is qualified to submit this thesis in application for that degree. I confirm that any appendices included in the thesis contain only material permitted by the 'Assessment of Postgraduate Research Students' policy.

Date 25 August 2021 Signature of supervisor

Permission for publication

In submitting this thesis to the University of St Andrews we understand that we are giving permission for it to be made available for use in accordance with the regulations of the University Library for the time being in force, subject to any copyright vested in the work not being affected thereby. We also understand, unless exempt by an award of an embargo as requested below, that the title and the

abstract will be published, and that a copy of the work may be made and supplied to any bona fide library or research worker, that this thesis will be electronically accessible for personal or research use and that the library has the right to migrate this thesis into new electronic forms as required to ensure continued access to the thesis.

I, Yahan Zhang, confirm that my thesis does not contain any third-party material that requires copyright clearance.

The following is an agreed request by candidate and supervisor regarding the publication of this thesis:

Printed copy

No embargo on print copy.

Electronic copy

No embargo on electronic copy.

Date 25 August 2021 Signature of candidate

Date 25 August 2021 Signature of supervisor

Underpinning Research Data or Digital Outputs

Candidate's declaration

I, Yahan Zhang, hereby certify that no requirements to deposit original research data or digital outputs apply to this thesis and that, where appropriate, secondary data used have been referenced in the full text of my thesis.

Date 25 August 2021 Signature of candidate

Acknowledgements

First of all, I would like to thank my supervisor Dr Gordon Florence who has given me a lot of support and encouragement. And he has been very patient with me, giving me enough time to learn new things and improve little by little. And I am grateful to him for being willing to let me stay in his group for my PhD.

I am also very grateful to Dr Rodrigo Freire De Araujo Gouy. He was very patient with me. I still remember that when I come to the lab in my first year, my English was very poor, but he was always very patient with me and gave me a lot of help. I am also very grateful to Callum Turner and Dr Marija Zacharova. Whenever I have problems, they always help me and give me advice. Thanks to Siyao Chen, my human translator, who always helped me to translate when I didn't understand some English. Thank you to my friend Shen Zhang who is always there for me when I am feeling down.

Thanks to Rebecca Wood, who helps me testing the bioactivity of compounds.

Finally, I would like to thank the staff at the University of St Andrews Chemistry Department NMR and MS services.

Abstract

Neglected tropical diseases (NTDs) are a group of infectious diseases that are endemic in tropical and subtropical regions.[1] The associated infectious agents include protozoa, bacteria, viruses, and helminth parasites. In particular, Human African Trypanosomiasis, Chagas disease and Leishmaniasis are responsible for high mortality and morbidity rates in developing countries. However, the current treatments for trypanosomiasis and leishmaniasis have severe side effects and can be lethal.[2] Most of these treatments are antiquated, resulting in emerging drug resistance, and are difficult to administer (mostly by injection). Therefore, there is an urgent demand to find safer, cheaper, and more efficient alternatives to the existing drugs. Natural products play an important part in drug discovery, with more than 50 % of modern drugs being directly or indirectly derived from them.[3] In particular, the natural product chamuvarinin was found to have potent activity against trypanosomatid parasites. In this project, we synthesized a series of chamuvarinin based analogues, aiming to expand the library of trypanosomatid inhibitors, and further exploring the structure-activity relationship (SAR).

Abbreviations

NTDs	**Neglected tropical diseases**
MDGs	**Millennium Development Goal**
HIV	**Human Immunodeficiency Virus**
AIDS	**Acquired Immune Deficiency Syndrome**
WHO	**World Health Organization**
DNDi	**Drugs for Neglected Disease initiative**
T. brucei	***Trypanosoma brucei***
BBB	**Blood-brain barrier**
T. cruzi	***Trypanosoma cruzi***
L. major	***Leishmania major***
VL	**Visceral leishmaniasis**
CL	**Cutaneous leishmaniasis**
ML	**Mucocutaneous leishmaniasis**
NECT	**Nifurtimox-Eflornithine combination therapy**
SAR	**Structure-activity relationship**
THP	**Tetrahydropyran**
THF	**Tetrahydrofuran**
EC_{50}	**Half maximal effective concentration**
SI	**Selectivity index**
BSF	**Bloodstream form**
µM	**Micrometers**
DMSO	**Dimethyl sulfoxide**
DCM	**Dichloromethane**
NEt_3	**Triethylamine**
NaAsc	**Sodium ascorbate**
RT	**Room temperature**
MeOH	**Methanol**
MsCl	**Methane sulfonyl chloride**
LAH	**Lithium aluminum hydride**
MeCN	**Acetonitrile**
Eq	**Equivalent**
Mp.	**Melting point**
h	**Hour**
NMR	**Nuclear Magnetic Resonance**
IR	**Infrared**
Hz	**Hertz**
s	**Singlet**
d	**Doublet**
t	**Triplet**
q	**Quartet**
dd	**Doublet of doublets**
td	**Triplet of doublets**
m	**Multiplet**
δ	**Delta**
J	**Coupling constant**
$CDCl_3$	**Chloroform**

mL	**Millilitre**
mmol	**Millimole**
mg	**milligram**
TBAF	**Tetrabutylammonium fluoride**
Ph	**Phenyl**
TPPO	**Triphenylphosphine oxide**
TPP	**Triphenylphosphine**
TBS	***tert*-Butyldimethylsilyl**
TBPB	***tert*-butyl peroxybenzoate**
EtOAc	**Ethyl Acetate**
Rf	**Retention factor**
M	**Moles per litre**
°C	**Degrees Celsius**

Contents

1. Introduction

1.1 Neglected tropical diseases

Neglected tropical diseases (NTDs) are a group of infectious diseases prevalent in tropical and subtropical regions.[1] The associated infectious agents include protozoa, bacteria, viruses, and helminth parasites.[1] There are four typical characteristics of NTDs: 1) people in poor areas are more vulnerable to infections because they lack good sanitation and adequate healthcare resources; 2) the majority of NTDs are chronic and can become increasingly severe if undetected and untreated over time; 3) NTDs may cause severe suffering and permanent disability, with long-term effects on patients and their families; 4) patients may often be excluded from society, which harms their mental health.[1]

These diseases are referred to as Neglected Tropical Diseases because they are ignored by policymakers. In 2000, the 'Millennium Development Goals' (MDGs) were declared by the United Nations aiming to reduce extreme poverty.[4] One of the goals outlined is to decrease the burden of three diseases: HIV/AIDS, malaria, and tuberculosis.[4] Therefore, the focus and funding have been heavily biased towards HIV/AIDS, malaria, and tuberculosis, leading to the overlooking of the other diseases, and thus contributing to higher mortality rates.

Recently, the awareness of NTDs has increased. Currently, a specific department within WHO aims to control and eradicate the NTDs, known as the Global Network for Neglected Tropical Disease Control.[5] The WHO also published their first report on NTDs and the treatments in 2010.[5] The quality of life of people living in the poorest areas can be greatly improved by making sufficient efforts to eradicate NTDs through following WHO guidelines.

1.2 Neglected tropical diseases caused by protozoa

Kinetoplastids are a group of flagellated protozoans, including *Trypanosoma* and *Leishmania*, which are responsible for several NTDs. *Trypanosoma brucei* causes Human African Trypanosomiasis, *Trypanosoma cruzi* is responsible for South American Trypanosomiasis, and *Leishmania spp.* cause leishmaniasis.[6] (Figure 1)

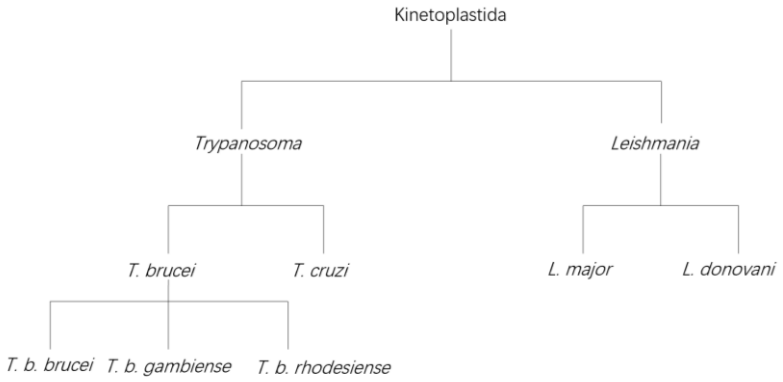

Figure 1 Kinetoplastida class

1.2.1 Human African Trypanosomiasis

Human African Trypanosomiasis (HAT), also referred to as sleeping sickness, is prevalent in sub-Saharan African countries and threatens more than 60 million people's lives.[6] The disease is transmitted by the vector insect (tsetse flies). When an infected fly takes a blood meal from a mammal host, the metacyclic trypomastigotes are injected into skin tissue from the salivary glands and pass into the bloodstream via the lymphatic system.[7] (Figure 2)

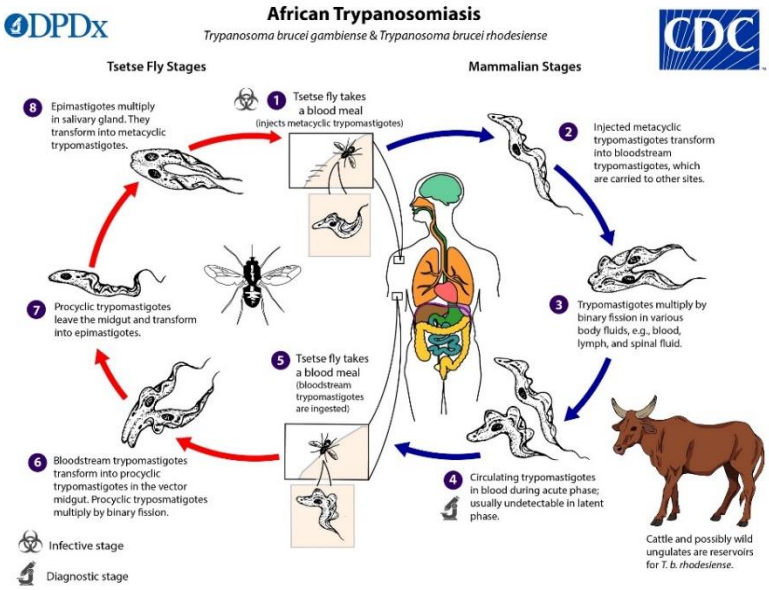

Figure 2 The life cycle of T. brucei in vector and host [8]

As HAT is most prevalent in poor African countries, some factors make access to treatment for this disease a challenge. Firstly, HAT heavily affects remote, impoverished areas with

weak health care systems, making early detection of infection challenging.[9] Secondly, the lack of expertise also limits the implementation of the initial diagnosis. Finally, limited government funding invested in treating the disease has resulted in pharmaceutical companies putting less effort into updating treatments.[9] However, recently these problems have been partially remedied by receiving funding and support from pharmaceutical companies. For example, Sanofi currently provides funding for diagnostics, new treatments and vector control.[9]

There are three subspecies of *T. brucei*: *T. brucei gambiense, T. brucei rhodesiense* and *T. brucei brucei*. The *T. brucei brucei* subspecies is the pathogen of animals.[10] Both *T. brucei gambiense* and *T. brucei rhodesiense* are pathogens causing HAT. Not only do they cause disease in different geographic regions, but they also lead to different types of HAT. The *T. b. gambiense* is predominant in Central and Western Africa and is more likely to cause chronic infections, whilst *T. b. rhodesiense is* predominant in Eastern and Southern Africa and causes acute infections.[10] In both cases of infections, the disease mainly undergoes two stages, the early haemolymphatic stage and the late encephalitic stage.[10] During the early haemolymphatic stage, the trypanosomes will enter the blood and lymphatic system, patients may develop headaches, fever, and joint pains. During the late encephalitic stage, the trypanosomes cross the blood-brain barrier (BBB) to invade the central nervous system, causing neurological and endocrinal disorders, and if left untreated, infected patients may die within a few months.[10]

1.2.2 American Trypanosomiasis

South American Trypanosomiasis also referred to as Chagas disease, is an endemic disease predominantly in Latin America, putting more than 25 million people at risk of infection with approximately 7 million people infected.[11] Recently, due to human migration and climate change, this disease has begun to spread North through central areas in the southern states of the USA.[11]

The causative agent of Chagas disease is *Trypanosoma cruzi (T. cruzi)*. Humans are infected with this parasite mainly through contact with the faeces of the infected triatomine bugs

(generally called kissing bugs).[11,12] When triatomine bugs suck the blood from a human, the faeces containing trypomastigotes are released close to the bite wound. Parasites enter the wound and multiply within the human body when people scratch the broken skin and move infected faecal droplets.[12] Additionally, *T. cruzi* also can be transmitted through non-vectorial methods, such as organ transplantation, blood transfusions and transplacentally.[12]

There are three distinct phases of Chagas disease: first is the acute stage, in which some patients may develop the symptoms of fatigue, fever, and swollen lymph nodes. It normally occurs in children and if left untreated, approximately 10% of symptomatic patients die of encephalomyelitis or severe heart failure.[12,13] The acute symptoms may spontaneously disappear after three to eight weeks and then be followed by an intermediate stage. This asymptomatic stage can last for decades or even a lifetime, making early diagnosis and treatment difficult.[12,13] Approximately 20% to 30% of infected people will enter the chronic stage. There are two different forms of the disease in this stage, one is cardiac complications, leading to heart failure, cardiac arrest, and enlargement of the heart; the other is gastrointestinal complications, which can cause damage to the digestive system, leading to the enlargement of the esophagus or colon.[12,13]

1.2.3 Leishmaniasis

Leishmaniasis is a spectrum of diseases caused by *Leishmania spp.* transmitted to humans through the bite of phlebotomine sandflies. When people are bitten by infected female sandflies, the promastigotes are injected into the host body via saliva and rapidly phagocytized by macrophages. Then promastigotes transformed into amastigotes and begin to divide and infect other cells. [14] According to the WHO report, more than 350 million people are at risk of infection, with approximately 1 million people infected with Leishmaniasis annually.[15]

Traditionally, according to the different geographic regions, leishmaniasis can be separated into two categories, one is the Old World, which is caused by the species found in African, Middle East and the Mediterranean countries, such as *L. infantum, L. donovani* and *L. major*. The other one is New World, which is caused by the species found in Central America, South

America, and Mexico, such as *L.mexicana*, *L.amazonenis*, and *L.braziliensis*.[14,15] The New World species cause visceral leishmaniasis (VL) and cutaneous leishmaniasis (CL), while the Old World species causes mucocutaneous leishmaniasis (ML).[14,15]

For visceral leishmaniasis also referred to as kala-azar, more than 95% of patients die if left untreated. Normally, symptoms of fever, weakness, and enlargement of lymph nodes develop within two to six months after the patient is infected. [14,16] Cutaneous leishmaniasis is the most common form of leishmaniasis, which causes more than 600,000 people to be infected each year.[16] Although cutaneous leishmaniasis is not fatal and people with strong immune systems even can spontaneously heal on their own, it can result in disfiguring scars and serious disability.[14,16] The mucocutaneous leishmaniasis usually occurs months or years after the first episode of cutaneous leishmaniasis, resulting in progressive damaging ulcers on the patient's mucous membranes extending from nose and mouth to pharynx and larynx.[16]

1.3 Current treatments

1.3.1 Treatments against HAT

The stages of the HAT and the subspecies of the parasite determine the choice of treatment. There are two drugs used for the early haemolymphatic stage: Pentamidine (**1**) and Suramin (**2**) (Figure 3). Pentamidine (**1**) has been used to treat *T. b. gambiense* HAT since 1940. However, the use of this drug usually results in low blood pressure and hypoglycemia in patients. Suramin (**2**) is used to treat *T. b. rhodesiense* HAT, which can cause side effects, such as renal failure, severe cutaneous reactions and neurotoxic symptoms.[2]

Three therapies are used to treat the encephalitic stage of HAT: Melarsoprol (**3**), Eflornithine (**4**), and the combination of Eflornithine (**4**) and Nifurtimox (**5**) (Figure 3). In the encephalitic stage of HAT, drugs are required to be able to cross the blood brain barrier, so they have to be relatively small molecules and are more lipid-soluble than the drugs used in the haemolymphatic stage. Melarsoprol (**3**) is an organo-arsenical compound and can effectively treat the last-stage *T. b. rhodesiense* HAT. However, the side-effects of Melarsoprol (**3**) are

severe, with 10% of patients developing reactive encephalopathy after treatment, half of whom eventually die.[17] Eflornithine (**4**) was initially used as a monotherapy for the treatment of *T. b. gambiense* HAT, and the Eflornithine (**4**) and Nifurtimox (**5**) combination therapy (NECT) was later approved in 2009. Compared to eflornithine monotherapy, NECT reduced the duration of treatment from 14 days to 10 days, and improved safety, decreasing the drug-related events from 29% to 14%.[18] Thus,NECT is used as the first-line treatment for *T. b. gambiense* HAT.[18] Although NECT treatment was a therapeutic improvement, the stage-specific and long-term administration (requiring prolonged intravenous infusions) restricts its usage.

Fexinidazole (**6**) is the first oral treatment for both haemolymphatic and encephalitic stage HAT, developed by the collaboration of Sanofi and the Drugs for Neglected Disease Initiative (DNDi).[19] In November 2018, the European Medicines Agency issued a positive opinion on the use of fexinidazole (**6**) for the treatment of HAT, which promoted the marketing authorization application of fexinidazole (**6**) in endemic countries. In December 2018, fexinidazole (**6**) was approved in the Republic of Congo, which has a high number of infections.[19] In July 2021, fexinidazole (**6**) was approved for medical use in the USA.[20] Compared to the other treatments, fexinidazole (**6**) is more convenient than other methods because it does not require prolonged intravenous infusions and definitive stage diagnosis.

	T. b. gambiense	*T. b rhodesiense*
Early stage	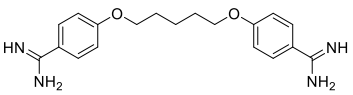 **1 Pentamidine**	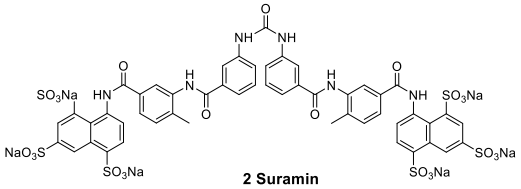 **2 Suramin**
Late-stage	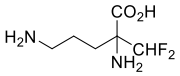 **4 Eflornithine** + 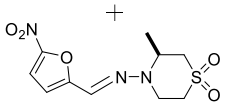 **5 Nifurtimox**	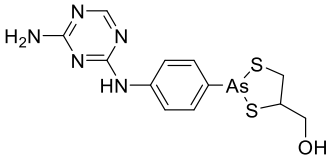 **3 Melarsoprol**
Both stages	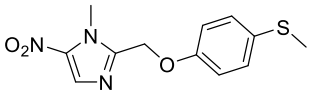 **6 Fexinidazole**	

Figure 3 Treatments against HAT[19,20]

1.3.2 Treatments against Chagas Disease

Currently, only two drugs are used to treat Chagas disease, namely Nifurtimox (**5**) and Benznidazole (**7**) (Figure 4). These two drugs have been on the market for over 40 years and are both administered orally.[21,22] Compared to Nifurtimox (**5**), Benznidazole (**7**) has better tolerability and a lower incidence of treatment discontinuations. Therefore, it is always used as the first-line treatment. However, their efficacy and safety profile are far from ideal, as both drugs can cause anorexia, muscle pain and sleeping disorders.[21,22]

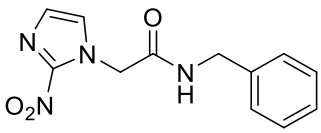

7 Benznidazole

Figure 4 Treatment against Chagas Disease[20]

1.3.3 Treatments against Leishmaniasis

There are five types of drugs used to treat leishmaniasis (Figure 5).[23] They are administered through different methods. Pentavalent antimony (sodium stibogluconate (**8**)) and Paromomycin (**10**) are administered by infusion, amphotericin B (**9**) and pentamidine (**1**) through intravenous, and miltefosine (**11**) is the only oral treatment. However, all these drugs have side effects, for example, amphotericin B (**9**) is nephrotoxic, and also expensive.[23]

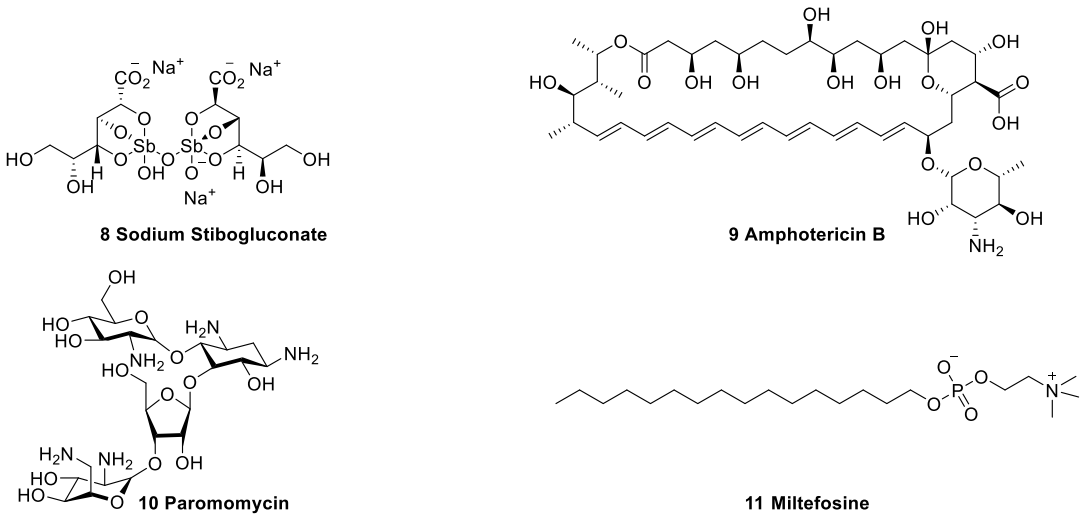

Figure 5 Treatments against Leishmaniasis[23]

In conclusion, most of these treatments are antiquated, resulting in emerging resistance, and are difficult to administer (mostly by injection). While a new human African trypanosomiasis drug Fexinidazole (**6**) has recently entered the market, it has been the only new drug developed for late-stage HAT in the last 30 years.[19] Thus, it is still necessary to find safer, cheaper and more efficient alternatives to the currently existing drugs.

1.4 Drug discovery strategies

The phenotypic and target-based screening approaches are the two main methods used in drug discovery. The specific protein chosen as a drug target needs to be validated first when using the target-based screening approach, followed by the design of a compound that can act selectively and effectively against the protein target.[24,25] The phenotypic screening methods include screening the compound libraries against the whole cells (or organisms), then the hit molecules are modified to further optimize the structure-activity relationship

(SAR). The next step is identifying the target through the chemical proteomics method.[24,25]

Both phenotypic and target-based screening approaches have their advantages and disadvantages. For the target-based screening approach, only the known target is used to screen the molecule libraries, so that the high quality SAR data can be obtained in the absence of other sources of interference.[24,25] However, when using the target-based approach, the selected molecule may have excellent activity against the target but have poor activity against the whole cells. This is because target-based screening is only based on a specific protein, and the complexity of the entire cell in terms of metabolism, molecular uptake, and molecular solubility is not considered. In addition, the incomplete knowledge of target proteins also limits the utility of this method.[24,25] When using phenotypic screening methods, the knowledge of the specific drug target is not required, so the molecule is evaluated in the biologically relevant environment, preventing the problem described above. However, it is a challenge to optimize the SAR in the absence of a known target.[24,25]

1.5 Natural products in drug discovery

The secondary metabolites produced by living organisms are defined as natural products.[26] Normally, secondary metabolites are produced to gain a proliferation advantage over other organisms, hence they are often toxic toward the surrounding organisms.[26] Since the natural products are synthesized through various biosynthetic pathways, the structure of these compounds is generally complex, resulting in strong biological activities in various types of cells.[26] Additionally, compared to most synthetic compounds, natural products and their medicinal derivatives regularly have more stereochemical centers and lower hydrophobicity, which not only benefit the pharmacokinetic parameters of drugs but also improve structure diversity.[26] The wide range of biological activity and structural complexity of natural products provide a good starting point in drug discovery. More than 50% of modern drugs are related to natural products.[27] Some natural products can be directly used for treatment without modification. For example, the antibiotic tetracycline is isolated from *Streptomyces aureofaciens*.[28] While, because of the toxic property of natural products, most of them cannot be directly used as a treatment for humans, about 44% of drugs currently on the

market are inspired by natural products.[27] In addition, total synthesis of natural compounds can be used in drug discovery, which solves the problems of low quantities of natural products in nature, providing a reliable source of the material.[27]

1.6 Natural products against Trypanosomatid parasites

1.6.1 Acetogenins

Acetogenins constitute a series of polyketide natural products, isolated from plants of the annonaceous species, which grow in tropical and sub-tropical regions.[29] Acetogenins normally consist of an unbranched C_{32} or C_{34} fatty acid backbone, ending in an α,β-unsaturated γ-lactone ring. Besides, the backbone chain may contain several oxygenated functions, like hydroxyls, tetrahydropyran (THP), and tetrahydrofuran (THF). [29,30] Over 400 acetogenins have been identified, and the majority of them show various biological activities, such as cytotoxic, pesticidal, and immunosuppressive properties.[29] In particular, acetogenins can interact with the electron transport chain, and are also established as potent mitochondrial Complex I inhibitors.[29]

Recently, several members of Annonaceous acetogenins have been identified to have activity against trypanosomatid parasites. (Figure 6) For example, Rolliniastatin **12** shows activity toward *T. cruzi,* with the EC_{50} value of 33 μM, and the EC_{50} value of Annonacin **13** is 69 μM.[29]

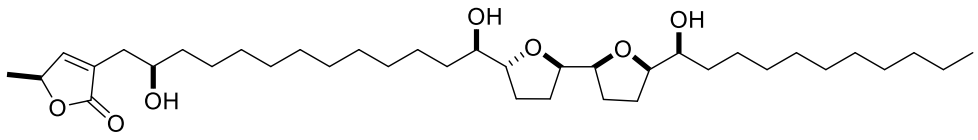

Rolliniastatin **12**, EC_{50}: 33 μM

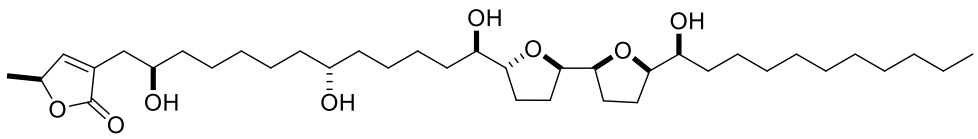

Annonacin **13**, EC_{50}: 69 μM

Figure 6 Products Against Trypanosomatid Parasites[29]

1.6.2 Chamuvarinin

In 2004, chamuvarinin (**14**) was extracted from *Uvaria chamae* by Laurens.[30] The total synthesis of Chamuvarinin (**14**) was first completed by the Florence group in 2011, reporting a 1.5% yield over 20 steps (Figure 7).[31] Structurally, Chamuvarinin (**14**) is an unusual acetogenin, containing a unique linked THF-THF-THP ring system. Like other acetogenins, chamuvarinin (**14**) also shows a range of biological activities, e.g. against KB3-1 cervix cancer cell line.[32]

The activity of chamuvarinin (**14**) against trypanosomatid parasites was tested by the collaboration between the Florence and Smith groups. These data revealed that chamuvarinin (**14**) showed potent trypanocidal activity toward *T. brucei*, with an EC_{50} value of 1.4 μM, and it also had potent cytotoxic effects on human Hela cells (Figure 7).[33]

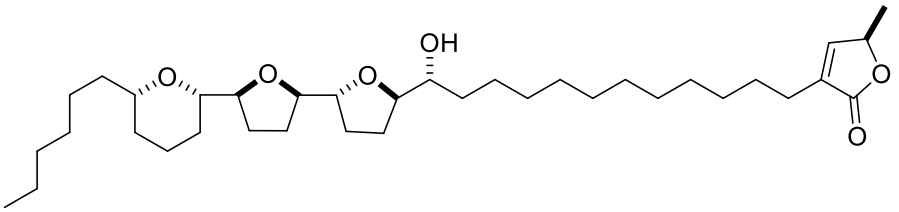

(+)-Chamuvarinin **14**
T.brucei EC_{50} 1.4 μM
HeLa EC_{50} 2.9 μM

Figure 7 Chamuvarinin structure[33]

Although acetogenins are known as Complex I inhibitors, the activity of chamuvarinin against trypanosomatid parasites cannot be explained by inhibition of complex I, as bloodstream *T.brucei* does not have a functional complex I and uses alternative ATP production pathways. Therefore, a different mode of action exists.[34]

1.7 Simplified analogues of Chamuvarinin

1.7.1 Outline of simplified analogues

While chamuvarinin (**14**) shows potent activity against trypanosomatid parasites, the research into the trypanocidal activity of chamuvarinin (**14**) has been limited. Therefore, Florence and Smith groups synthesized a series of analogues based on the chamuvarinin

structure.[35,36] The phenotypic screening based synthetic method was used to maximise the activity of trypanocidal compounds. The new designed trypanocidal inhibitors not only had reduced structural complexity compared to chamuvarinin (**14**) but also preserved its trypanocidal activity.

1.7.2 Triazole containing analogues

In order to reduce the structural complexity of chamuvarinin (**14**), molecular modelling was used to investigate the favorable orientation of chamuvarinin. The molecular modelling of the central tricyclic core of chamuvarinin reveal that the molecule has the lowest energy when the central core adopts the 'U-shaped' conformation (Figure 8).[35] Thus, compounds that adopted a similar 'U-shaped' conformation were hypothesized to have similar biological properties.[35]

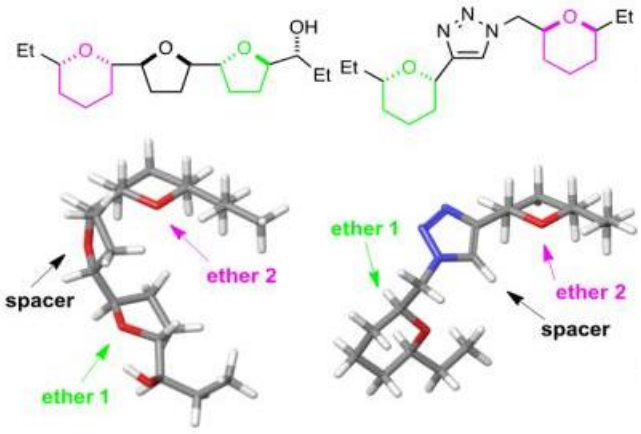

Figure 8 Lowest energy conformation of the central tricyclic core[35]

Therefore, the 1,4-triazole motif was used as a spatial mimic for the central tetrahydrofuran (THF) motif found in chamuvarinin. In addition, another synthetically challenging THF ring was replaced with a more easily readily accessible tetrahydropyran (THP) motif. The central triazole spacer was introduced via the copper-catalyzed 1,3-dipolar cycloaddition of azide **15** and alkyne **16**. Thus, the complex structure of the chamuvarinin heterocyclic core inspired the THF-triazole-THF structure (Figure 9).[35]

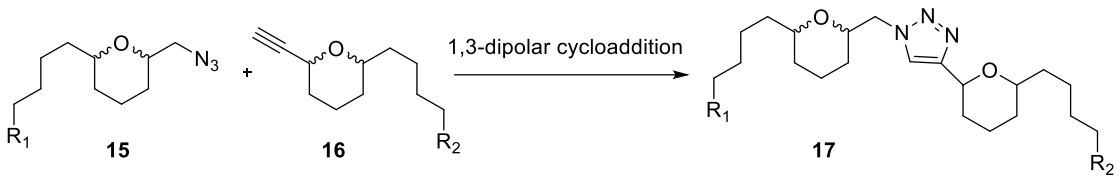

Figure 9 THF-triazole-THF contained analogue design[35]

The first series of analogues were synthesized based on this core structure. The biological activities results of the **18-29** series are shown in Table 1.[35] The biological data revealed that the stereochemistry of each THP influenced the trypanocidal activity of the compound. In the R_1, R_2= Et, Et and R_1, R_2= Et, OBn series, the *syn-anti* analogues **19** (entry 2) and **24** (entry 7) were the most active compound, while in the R_1, R_2= Et, OH serious, the *syn-syn* analogue **25** (entry 9) proved the most active. Among these three types of analogues, compound **26** had the highest activity against *T.brucei* (EC_{50} 1.8 μM), which is very similar to chamuvarinin (**14**) (EC_{50} 1.4 μM). Thus, compound **26** became the lead compound for further optimization.

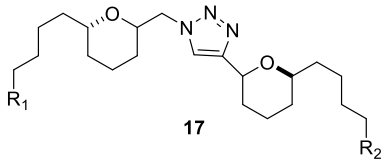

Entry	Compound	R1-THP-THP-R2	*T.brucei* (BSF) EC_{50} (μM)	HeLa EC_{50} (μM)	Selectivity Index (*T.brucei* vs Hela)
1	**18**	Et-*syn*-*syn*-Et	48.7±3.5	>100	>2
2	**19**	Et-*syn*-*anti*-Et	7.6±0.3	166.6±18.0	5.3
3	**20**	Et-*anti*-*syn*-Et	37.2±6.6	>500	>6
4	**21**	Et-*anti*-*anti*-Et	24.6±1.4	33.0±2.4	1.3
5	**22**	Et-*syn*-*syn*-OBn	8.7±0.5	45.5±2.5	5.3
6	**23**	Et-*syn*-*anti*-OBn	10.1±0.4	76.0±3.0	7.5
7	**24**	Et-*anti*-*syn*-OBn	3.1±0.1	71.4±4.1	23
8	**25**	Et-*anti*-*anti*-OBn	4627.2±40.3	>1000	>2
9	**26**	Et-*syn*-*syn*-OH	1.8±0.1	7.0±1.0	3.9
10	**27**	Et-*syn*-*anti*-OH	17.5±1.0	26.9±1.1	1.5
11	**28**	Et-*anti*-*syn*-OH	72.4±3.9	59.7±2.5	0.8
12	**29**	Et-*anti*-*anti*-OH	223.2±21.8	415.8±35.3	1.9

Table 1 Biological data for compounds 18-29[35]

1.7.3 Substituted THP series

The limited number of possible triazole based analogues restricted the further exploration of SAR, therefore, introducing substituent in THP ring was used to expand the library of trypanocidal inhibitors. Position 4 was chosen because it is spatially directed away from the central triazole core, which is most likely to be involved in inhibitor-protein binding interactions.[36]

A series of compounds containing a 4-substituted THP motif were synthesized. The biological results are shown in Table 2.[36] Most of the analogues had excellent activity against *T. brucei* (EC_{50}< 10). A very obvious trend was that the increased length of the alkyl chain had a positive influence on selectivity, in particular, the SI of compound **32** (entry 3) was over 130.

In addition, through photoaffinity labelling, Complex V was identified as a new target for the simplified compound.[34]

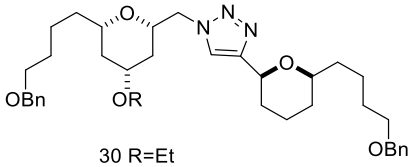

30 R=Et
31 R=Pr
32 R=Bu
33 R=Bn

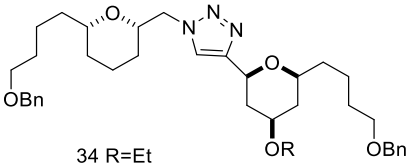

34 R=Et
35 R=Pr
36 R=Bu
37 R=Bn

Entry	Compound	*T.brucei* (BSF) EC_{50} (μM)	HeLa EC_{50} (μM)	Selectivity Index (*T.brucei* vs Hela)
1	**30**	5.1±0.3	21.1±5.3	4.1
2	**31**	6.3±0.5	43.2±7.3	6.9
3	**32**	3.8±0.1	>500	>130
4	**33**	5.2±0.5	>500	96
5	**34**	5.8±0.5	53.6±5.3	9.2
6	**35**	7.4±0.4	>500	>67
7	**36**	4.8±0.4	>500	>104
8	**37**	5.0±0.2	>500	>100

Table 2 biological data for compound 30-37 [36]

1.7.4 Molecular modelling

Molecular docking is a method for predicting the favorable orientation of ligands in stable

complexes with proteins by computationally simulating the molecular recognition process.[37] The lowest energy complexes of proteins and ligands can be obtained by calculating the chemical potential of the molecule. Molecular docking plays an important role in drug discovery, as it can be used to determine which structures can be simplified and still maintain a similar level of binding affinity to the original compound.[37]

1.7.5 Biphenyl containing analogues

After completing the THP-triazole-THP based series, further simplification of the scaffold by reducing the number of stereocenters was achieved. Through molecular docking experiments, using both bovine Complex V and the *T. brucei* Complex V, obtained from the X-ray models, it was identified that the biphenyl motif could be used to replace the unsubstituted half of the molecule. Therefore, a series of compounds based on the THP-triazole-biphenyl scaffold was synthesized. The biological results are showed in Table 3.[38] All the THP-triazole-biphenyl scaffold-based compounds not only show good activity against *T. brucei* but also had excellent selectivity. The length of the linker between biphenyl and triazole had little influence on the activity of the compound against *T. brucei* and Hela cells (entry 1,2,3), but the two-carbon linker had broad range activity, as the compound **39** (entry 2) with a 2-carbon linker was the only one of the three compounds that had activity against *T.cruzi*.

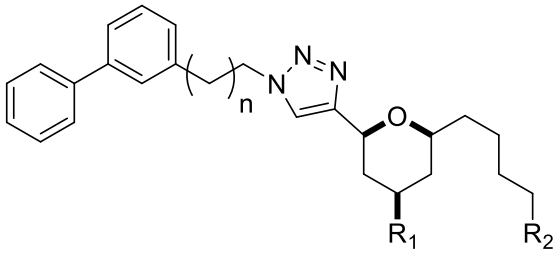

Entry	Compound	n,R_1,R_2	*T.brucei* (BSF) EC_{50} (μM)	*T.cruzi* EC_{50} (μM)	*L.major* EC_{50} (μM)	HeLa EC_{50} (μM)	Selectivit Index (*T.bruce* vs Hela)
1	**38**	0,O*n*Pr, OBn	8.2±0.3	>500	>500	>500	>60
2	**39**	1,O*n*Pr, OBn	7.5±0.2	35.2±10.0	>500	>500	>66
3	**40**	2,O*n*Pr, OBn	5.1±0.2	>500	>500	118.8±6.0	>23
4	**41**	1,O*n*Pr, O*n*Bu	8.7±0.3	16.8±1.1	52.3±5.0	>500	>57
5	**42**	1,OEt, OBn	5.6±0.2	10.9±0.8	>500	>500	>89
6	**43**	1,OEt, O*n*Bu	6.8±0.2	18.5±0.7	31.4±0.4	43.4±3.7	6.4

Table 3 biological data for compound 38-43[38]

1.7.6 Terminal benzene substituted series

Using compound **42** as the lead compound, Zacharova introduced different substitutions in the terminal phenyl ring. The biological results are shown in Table 4.[39] All the compounds not only show potent activity against *T. brucei*, with EC_{50}< 10 μM but also have excellent selectivity against HeLa cell line with SI > 10. Compound **47** (Entry 5) is the most potent inhibitor, the activity of this compound is very close to chamuvarinin (**14**) (*T. brucei* EC_{50} 1.4 μM, HeLa EC_{50} 2.9 μM), and the selectivity against the HeLa cell line is almost 18 times better.

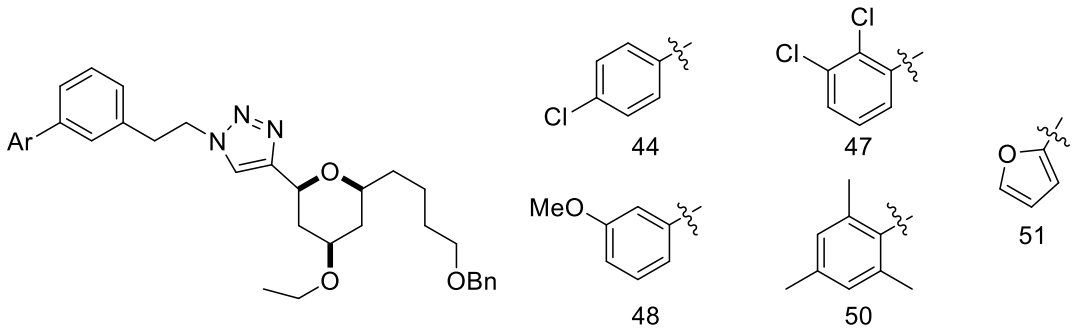

compound 42

Entry	Compd	*T.brucei* (BSF) EC_{50} (μM)	*T.cruzi* EC_{50} (μM)	*L.major* EC_{50} (μM)	HeLa EC_{50} (μM)	Selectivity Index (*T.brucei* vs Hela)
1	**44**	8.1±0.3	162.0±42.0	>250	>250	>31
2	**45**	2.6±0.2	41.2±8.8	172.0±20.0	>250	>96
3	**46**	3.3±0.2	9.7±1.4	39.0±2.1	>250	>76
4	**47**	1.8±0.1	47.1±8.9	62.9±2.6	98.1±26.7	54.5
5	**48**	4.6±0.2	88.1±35.1	60.3±11.9	>250	>54
6	**49**	6.3±0.4	52.2±16.1	144.0±28.9	>250	>40
7	**50**	4.5±0.4	21.4±4.0	>250	>250	>56
8	**51**	6.2±0.4	4.1±0.5	14.9±1.7	63.5±15.2	>10.2

Table 4 biological data for compound 44-51[39]

1.7.7 Mammal Scaffold Inhibitors : initial leads

In order to further reduce the structural complexity of the compounds, Florence group proposed a further simplified scaffold with different heterocycle rings replacing the THF substituted ring.[39] The biological results are shown in Table 5. Compound **52** not only showed good activity against *T. brucei* but also had good selectivity against the Hela cell line. However, it did not show good activity towards *T. brucei* and *L. major*. Nevertheless, compound **52** deserved further investigation and optimization of bioactivity.

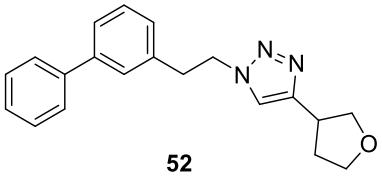

52

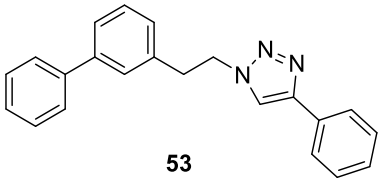

53

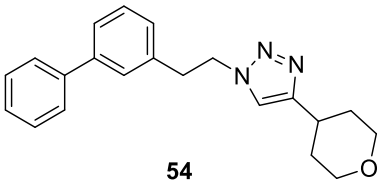

54

Entry	Compd	*T.brucei* (BSF) EC_{50} (μM)	*T.cruzi* EC_{50} (μM)	*L.major* EC_{50} (μM)	HeLa EC_{50} (μM)	Selectivity Index (*T.brucei* vs Hela)
1	**52**	3.17±0.18	46.1±5.4	117±3.0	80.5±5.8	25.4
2	**53**	15.0±0.8	>250	>250	>250	>16
3	**54**	29.0±1.6	115±18	>250	72.5±19.6	2.5

Table 5 biological data for compound 52-54[40]

1.8 Aims

In this project, we intended to investigate the effect of introducing modification into the lead compound **52**, to get a deep insight into the structure-activity relationship. Different modification strategies are shown below (Figure 10):

1) Introducing different substitutions into the terminal ring
2) Replacing the terminal benzene ring with the heterocycles
3) Replacing the terminal THF ring with the furan ring

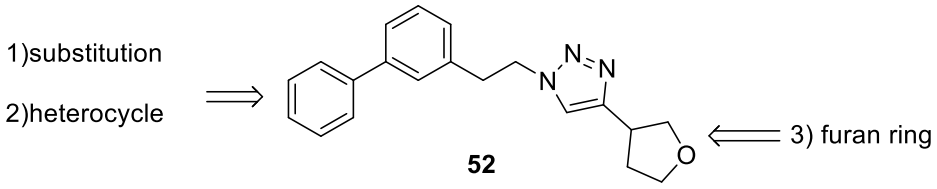

Figure 10 different modification strategies

By comparing the trypanocidal activity of previously synthesized compounds (Table 4), introducing a 2,3-dichloro substituent on the terminal benzene ring gave the best activity

against *T.brucei*, hence target compound **55** was designed. Also, replacing the terminal benzene ring with the THF ring, resulted in potent activity against *T.cruzi* (entry 8, Table 4), therefore, the compound **56** was designed. To further observe the effect of the chiral center on the activity of the compound, the achiral compounds **57** and **58** were selected for synthesis (Figure 11). This project aims to synthesize these four main leading compounds which are predicted to have good trypanocidal activities.

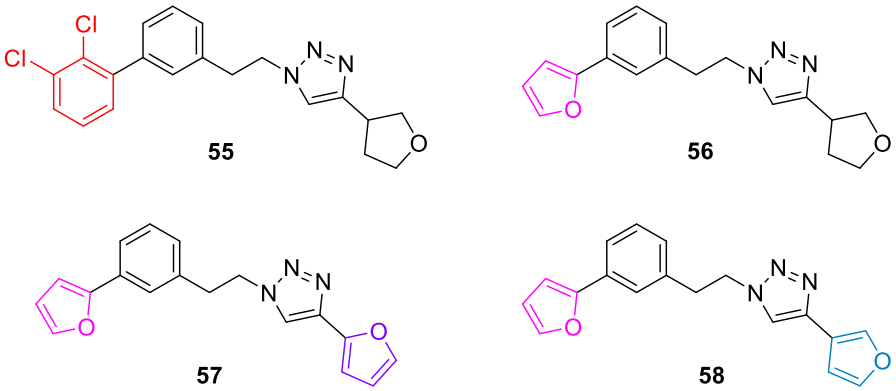

Figure 11 Target compounds

2. Results and Discussion

2.1 Synthesis strategy for the leading compounds 55 and 56

Two different synthetic routes were designed for synthesizing compounds **55** and **56**. The first synthetic route introduced the aromatic ring at the last stage. The retrosynthetic analysis for THF-triazole based analogues is shown in Scheme 1. Firstly, the copper-catalyzed 1,3-dipolar cycloaddition of azide and alkyne would give the central triazole spacer. Substituted aryl groups or heterocycles can be introduced via a Pd-catalyzed cross coupling reaction or related coupling reaction.

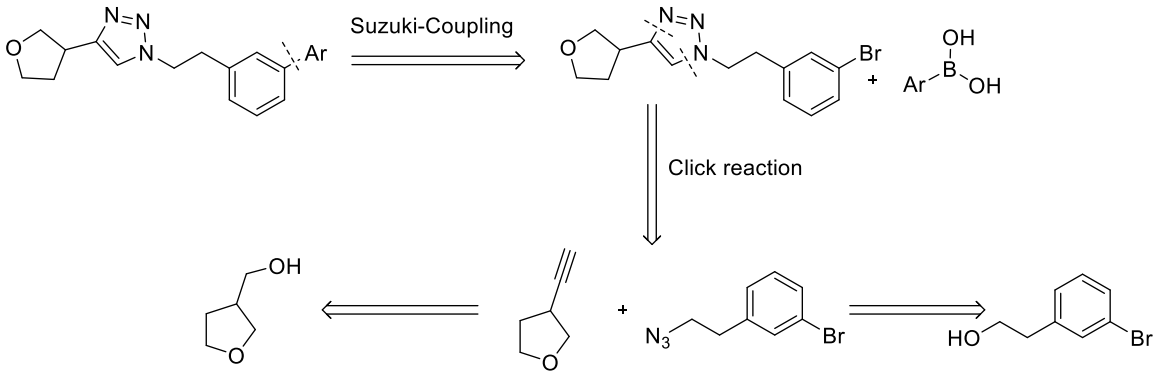

Scheme 1 Route 1 retrosynthetic strategy

The second synthetic route introduced the aromatic ring at an early stage. The retrosynthetic analysis for THF-triazole based analogues is shown in Scheme 2.

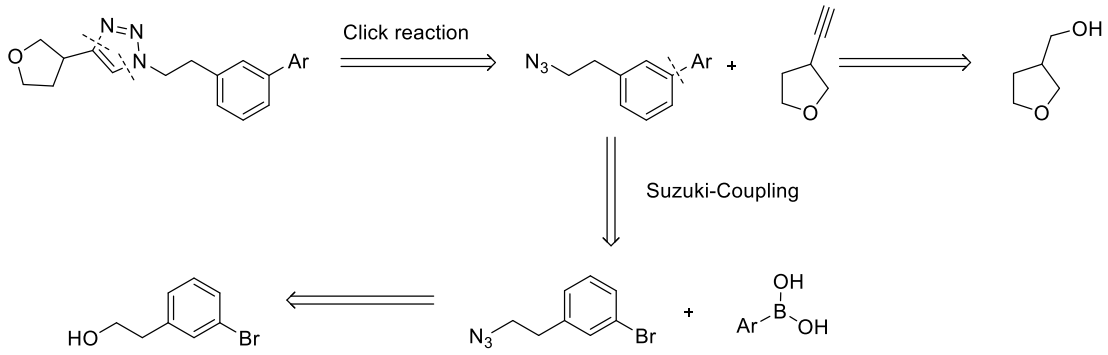

Scheme 2 Route 2 retrosynthetic strategy

2.2 Synthesis of compound 55 via route 1

2.2.1 Synthesis of aldehyde Compound **57**

The aldehyde compound **57** was synthesized via Swern oxidation. In the reaction, DMSO firstly reacts with oxalyl chloride producing the reactive species dimethylchlorosulfonium ion intermediate, followed by the reaction of alcohol compound **56** to produce the alkoxysulfonium ion. Then triethylamine as the base deprotonates the alkoxysulfonium ion, yielding the sulfur ylide. Finally, the decomposition of sulfur ylide gives the desired aldehyde compound **57**. Due to the volatility of the compound, it was carried to the next step without further purification.

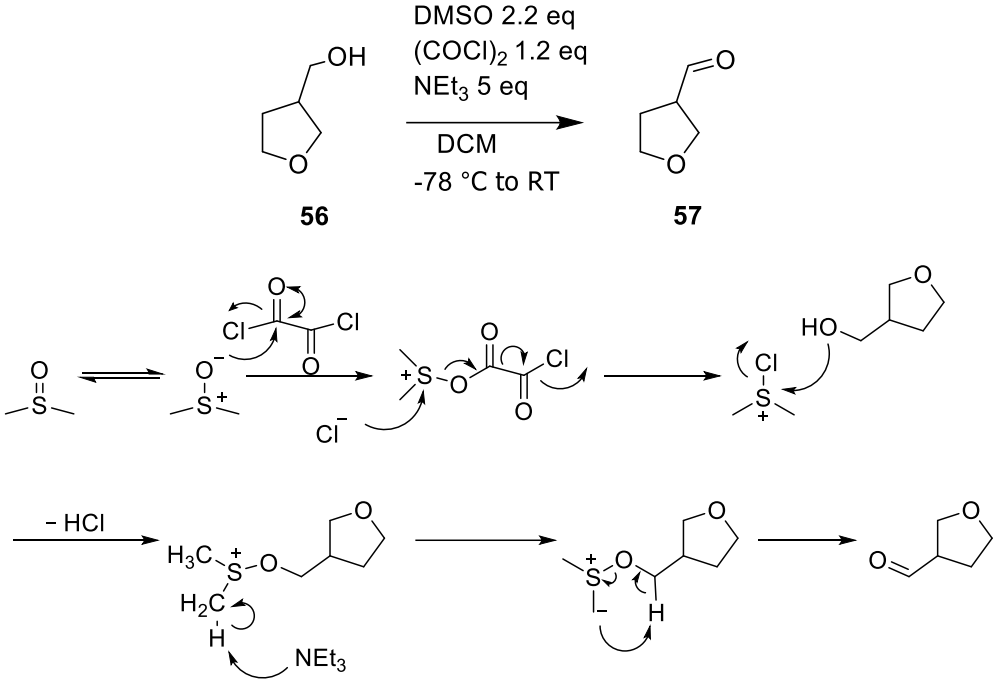

Scheme 3 Mechanism for Swern Oxidation

2.2.2 Synthesis of Ohira Bestmann Reagent **59**

The Ohira Bestmann reagent was synthesized via diazo transfer reaction. The sodium hydride is used as a base to deprotonate the alpha acidic hydrogen. The possible mechanism is shown in Scheme 4.

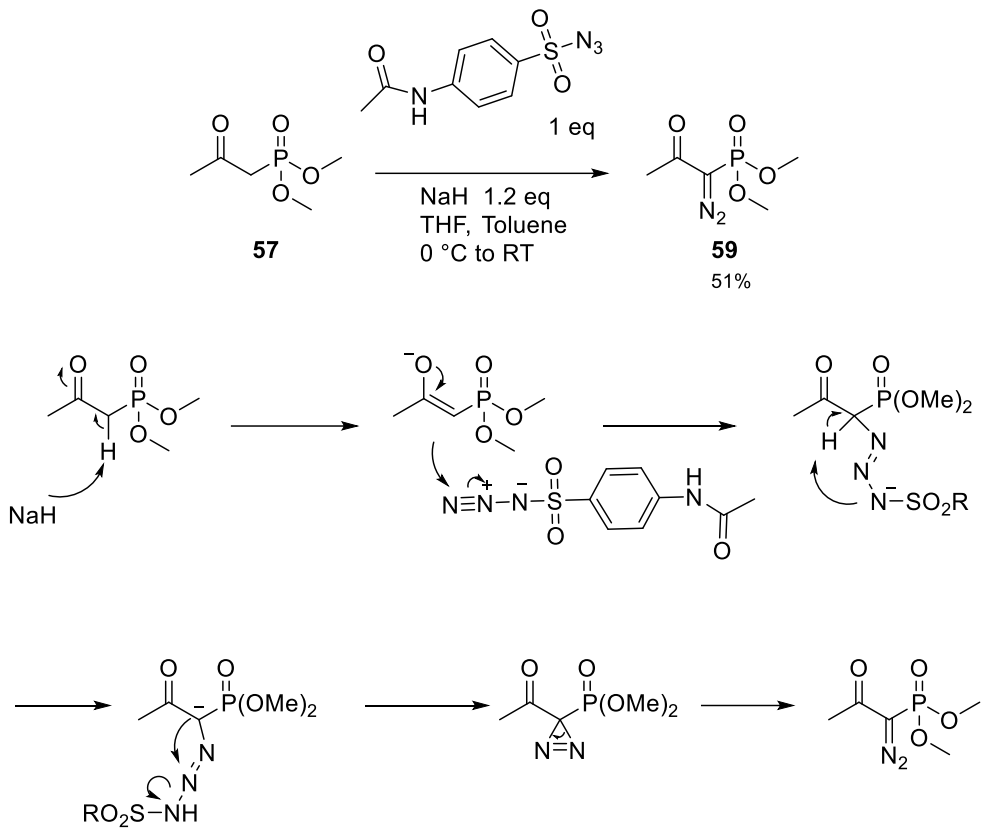

*Scheme 4 Mechanism for compound **59***

2.2.3 Synthesis of alkyne compound **60**

Alkyne **60** is obtained by Seyferth-Gilbert homologation of aldehyde compound **57**. For this reaction, the deprotonated methanol attacks the Ohira-Bestmann reagent, forming a nucleophilic intermediate, which then attacks the ketone compound **57**, obtaining the oxaphosphetane. Through a series of intramolecular reactions, the carbene intermediate forms. The desired compound **60** is formed via 1,2 migration. Due to the volatility of the compound, it was carried to the next step without further purification.

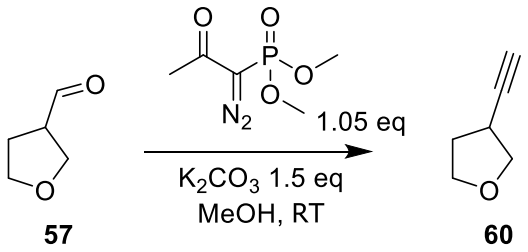

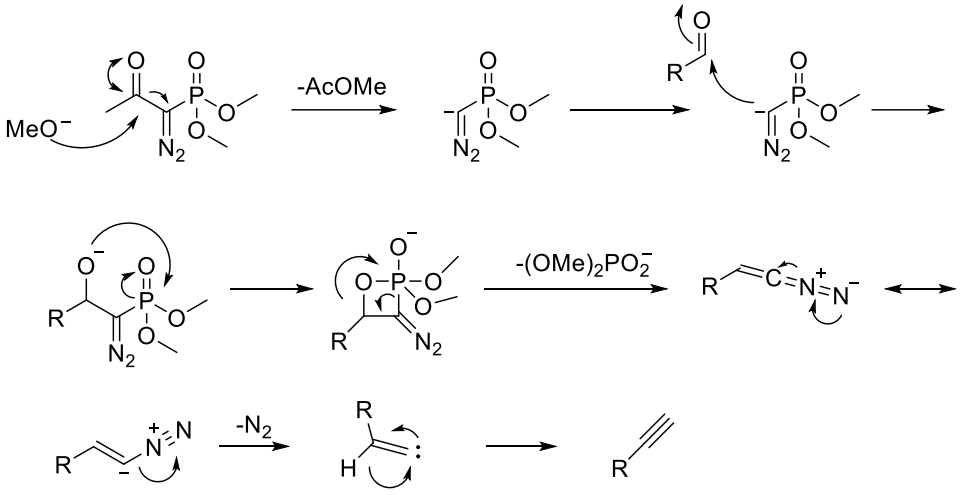

*Scheme 5 Possible mechanism for synthesis compound **60***

2.2.4 Synthesis of compound **62**

Synthesis of compound **62** was achieved in two steps. In the first step, deprotonated alcohol reacted with methanesulfonyl chloride to get the intermediate compound containing the good leaving methanesulfonyl group. In the second step, the mesylate reacts with sodium azide via S_N2 reaction to achieve the desired compound **62**.

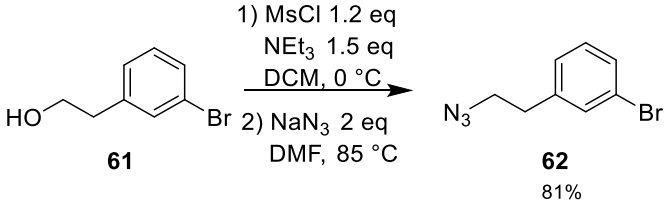

*Scheme 6 Synthesis of compound **62***

2.2.5 Synthesis of triazole compound **63**

The copper-catalyzed 1,3-dipolar cycloaddition was used to synthesize the triazole compound **63**. The sodium ascorbate is the reducing agent to reduce the Cu(II) to the active Cu(I). The mechanism is shown in Scheme 7.[41]

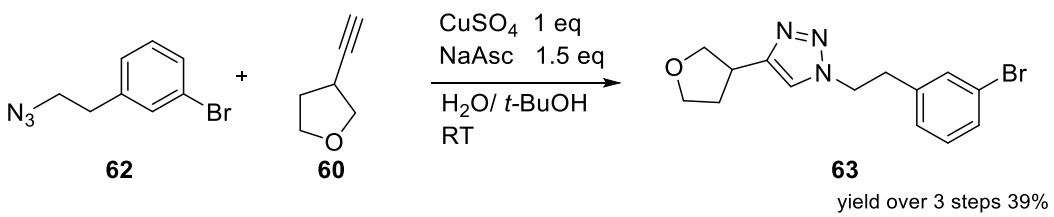

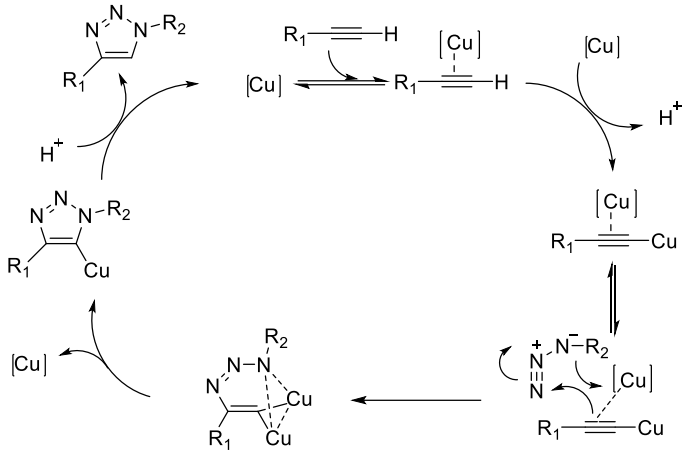

Scheme 7 Mechanism for click chemistry reaction[41]

2.2.6 Synthesis of compound **55**

For the final step, Suzuki-Miyaura coupling reaction was used to introduce the dichloro-substituted aryl ring, using tetrakis(triphenylphosphine) palladium as a catalyst. The mechanism is shown in scheme 8.[42] The catalytic cycle starts with oxidative addition of the aryl halide. Then the complex reacts with the base, forming the Ar-Pd$^{(II)}$-OH species. Next, the generated species reacts with activated aryl boronic acid via the transmetalation step, forming the Ar-Pd$^{(II)}$-Ar species. Finally, the Pd$^{(II)}$ species undergoes the reductive elimination, giving the desired compound **55** and Pd$^{(0)}$catalyst is regenerated.

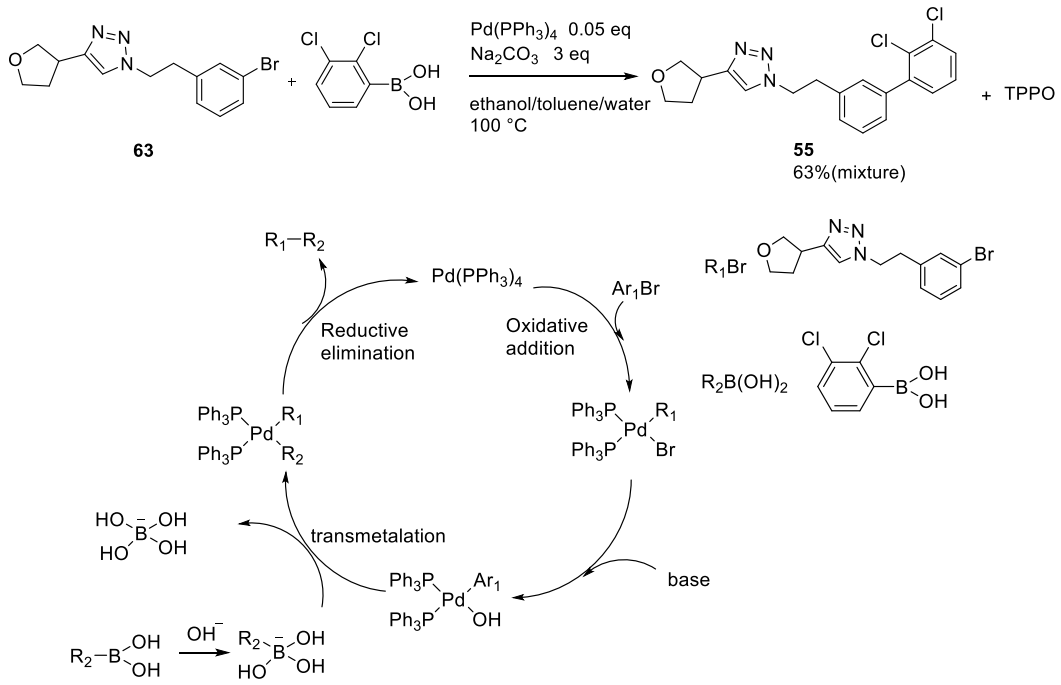

Scheme 8 Possible mechanism for the Suzuki-Miyaura coupling reaction[42]

However, when using the tetrakis(triphenylphosphine) palladium as a catalyst, the inseparable byproduct triphenylphosphine oxide (TPPO) was formed. Therefore, different methods were tried to separate the TPPO. According to the literature, TPPO reaction with zinc chloride can form the TPPO-Zn precipitate, which can be used to remove the TPPO byproduct (Scheme 9).[43] However, the TPPO byproduct was not removed using this method, possibly because this method was not suitable for the small scale reactions.

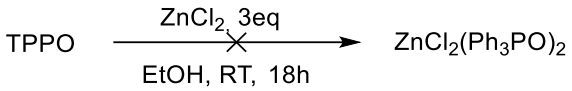

Scheme 9 Forming TPPO-Zn precipitates

Then different catalysts which do not contain TPP ligand were screened (Table 6). A new problem arose, the debromination compound **65** was synthesized, which also had similar polarity as the desired product **55** (Figure 12). Although changing catalyst influences the proportion of desired product and debrominated product, none of these catalysts can avoid the formation of debrominated products (Table 6). The formation of debrominated compound **65** is probably due to the slow transmetalation step, causing the intermediate Ar-Pd-Br species to obtain a proton from the solvent and replace the bromine to form the Ar-Pd-H species, and this species then goes through the reductive elimination step to form the final debromination compound **65**.

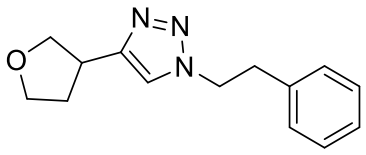

65

Figure 12 Debromination product 65

catalyst	ligand	Product: byproduct
Pd (dppf)Cl_2		1:1.5
$Pd_2(dba)_3$	XPhos	1:1
	SPhos	1:8
	JohnPhos	1:2

Table 6 The results of screening different catalysts

In order to change the polarity of the product to stop it from co-eluting with the debromination byproduct, introduction of the aryl ring was tried before the triazole formation step (Scheme 10). However, this resulted in decomposition, probably because the azide **62** was unstable to the high temperatures employed.

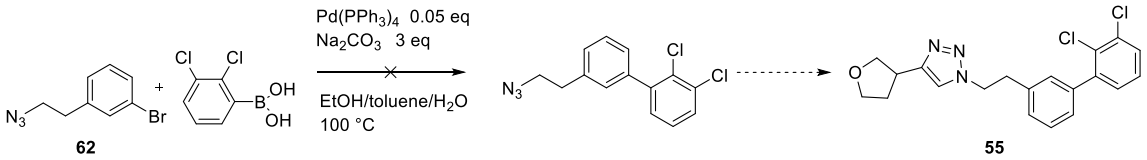

Scheme 10 Possible synthetic route

2.3 Synthesis of compound 55 via route 2

2.3.1 Introducing the aromatic ring at an early stage

For synthetic route 2, the aromatic ring is introduced at the early stage via Suzuki coupling reaction. Firstly 3-bromophenethyl alcohol **61** reacted with dichlorophenylboronic acid to afford the desired compound **66**, however, the final product was mixed with unknown byproducts (Scheme 11). As the mass spectrum in this step showed a mixture of unidentified products, it was not analyzed what the byproducts were. The mixture was then directly used in the next step in an attempt to separate the byproducts in the next step. However, the byproducts still could not be separated after the final step. The debrominated compound **67** was identified by analyzing the mass spectrum of the mixture in the last step.

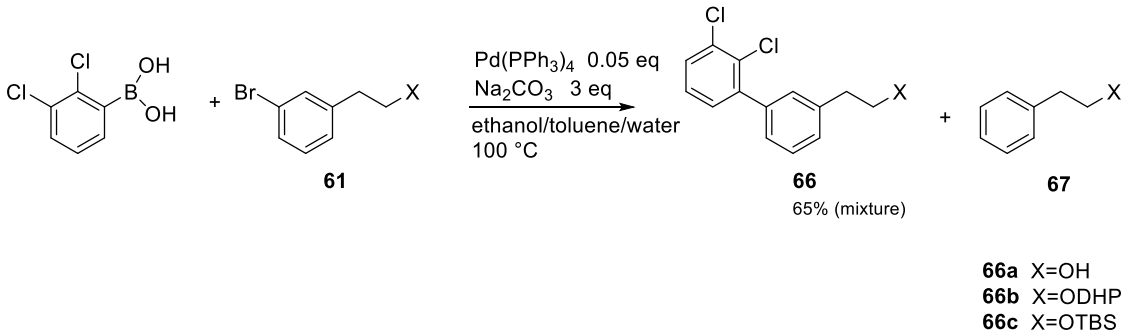

Scheme 11 Synthesis of compound 66

Compound	Ratio
66a:67a	2:1
66b:67b	6:1
66c:67c	10:1

Table 7 The results of using different protecting group

To avoid co-elution, different alcohol protecting groups were introduced to alter the polarity of the compound **61** (Shown in Table 7). The protected compound reacted with dichlorophenylboronic acid, thereby introducing the aromatic ring. This revealed that introducing protecting group reduced the formation of debrominated byproduct as well as allowed the debrominated byproduct to be isolated. Also, the *tert*-butylsilyl (TBS) protection group was more effective than dihydropyran (DHP) protecting group.

2.3.2 Subsequent steps for the synthesis of compound **55**

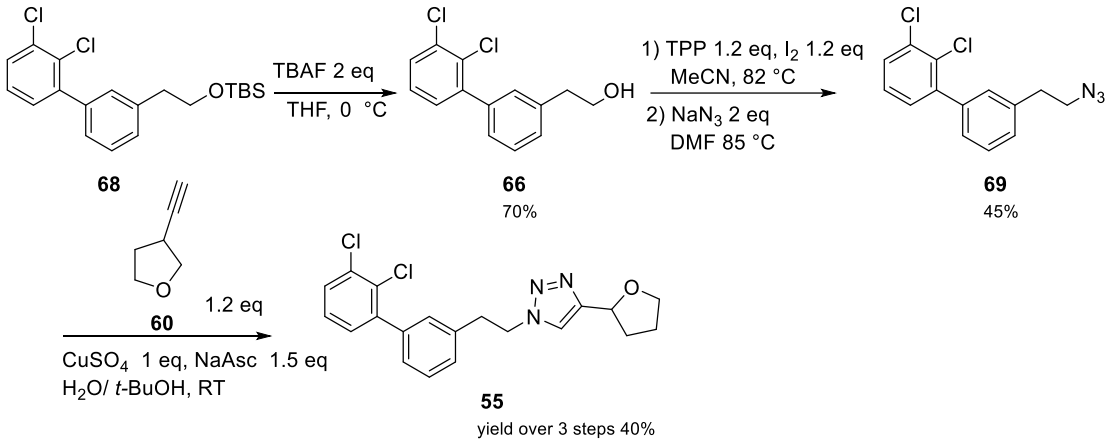

Scheme 12 Subsequent steps in the synthesis of compound 55

For the next few steps, tetrabutylammonium fluoride was used to remove the silyl ether protecting group, obtaining the deprotected alcohol **66**. Then triphenylphosphine and iodine were used to activate the alcohol, turning it into the good leaving group. After that, sodium azide reacted with alkyl iodide via S_N2 reaction to give azide **69**. In the final step, azide **69** reacted with alkyne **60** via copper-catalyzed 1,3-dipolar cycloaddition, yielding the desired compound **55**.

2.4 Synthesis of compound 56 via route 2

2.4.1 Introducing the furan ring via different coupling reactions

In order to introduce the furan ring, the Suzuki coupling reaction was first attempted. However, only the debromination compound **72** was obtained. Hence, the temperature was lowered from 100°C to 60°C and the proportion of boric acid was increased from 1.5 eq. to 3 eq. in an attempt to optimize this reaction, but only debromination compound **72** was observed.

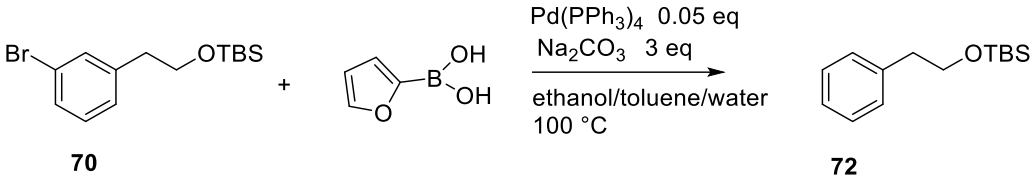

Scheme 11 Introducing the furan ring via Suzuki coupling reaction

Therefore, the Negishi coupling was attempted to introduce the furan ring. The first step was to deprotonate the furan and then transmetallate with zinc iodine to synthesize the Negishi reagent, then directly adding it to the solution of compound **70**. However, no reaction was observed (Scheme 14).

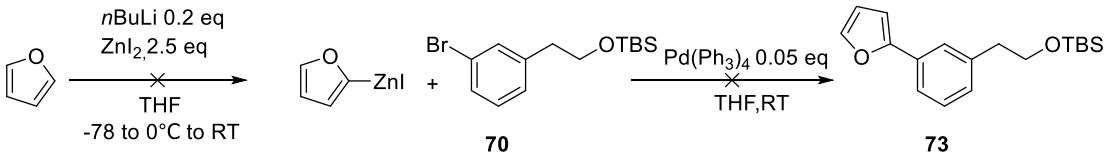

Scheme 14 Introducing the furan ring via Negishi coupling reaction

The Stille coupling reaction was then used to introduce the furan ring. This reaction is less water sensitive than Negishi coupling. Compound **70** reacted with the 2-(tributylstannyl) furan, yielding the desired compound **73**.

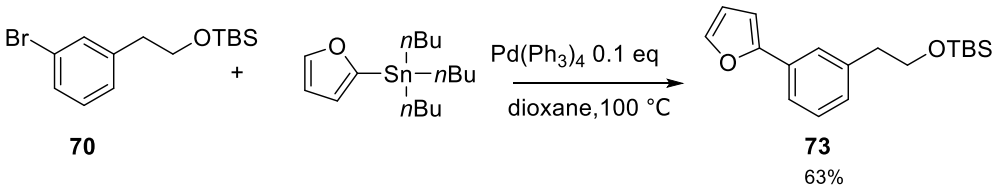

Scheme 15 Introducing the furan ring via Stille coupling reaction

When using the Stille coupling reaction to introduce the furan ring, the debromination byproduct was not observed. Therefore, introduction of the furan ring was attempted using Stille coupling reaction. However, the tributyltin bromide formed and could not be separated

from the desired compound **56** (Scheme 16).

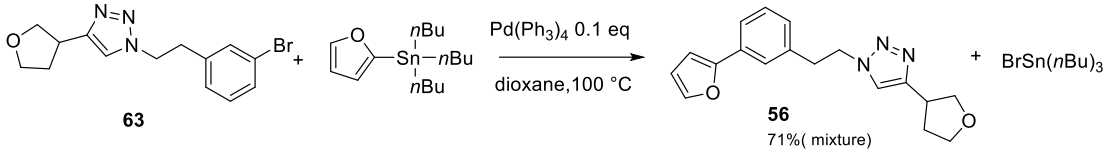

Scheme 16 Introducing the furan ring via Stille coupling reaction

2.4.2 Subsequent steps for the synthesis of compound **56**

TBAF was used to remove the TBS protecting group in compound **73**, obtaining the deprotected alcohol compound **75**. The aldehyde was converted into the iodide which then reacted with sodium azide via S_N2 reaction yielding the azide **76**. In the final step, azide **76** reacted with alkyne **60** via copper-catalyzed 1,3-dipolar cycloaddition, obtaining the desired compound **56**.

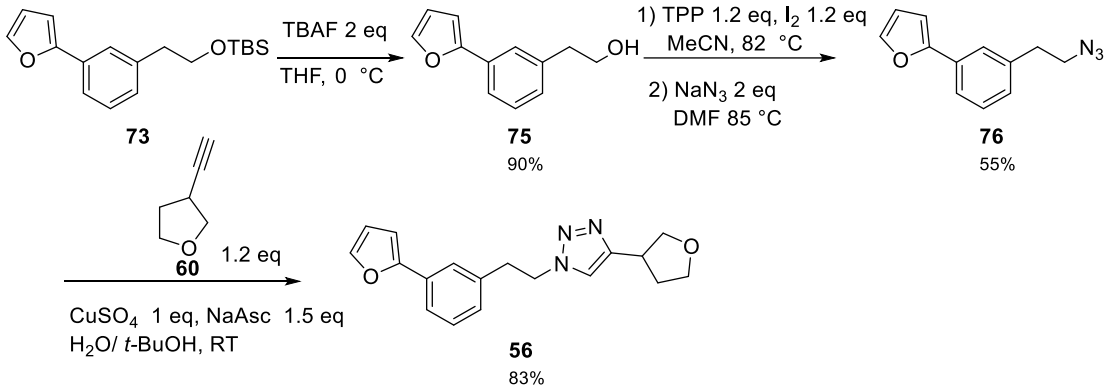

*Scheme 17 Subsequent steps in the synthesis of compound **56***

2.5 Synthetic route of compounds 57 and 58

Synthesis of compound **57** is shown below (Scheme 18). In the first step, the carboxylic acid **77** was reduced to alcohol **78** using LAH. The alcohol **78** was then oxidized to the aldehyde **79** using MnO_2. Next, aldehyde **79** reacted with Ohira-Bestmann regent **59** to yield alkyne **80**. In the final step, alkyne reacted with azide **76** in the cycloaddition reaction, providing the desired compound **57**. The synthetic route of compound **58** was the same as that of compound **57** except that different carboxylic acid was used.

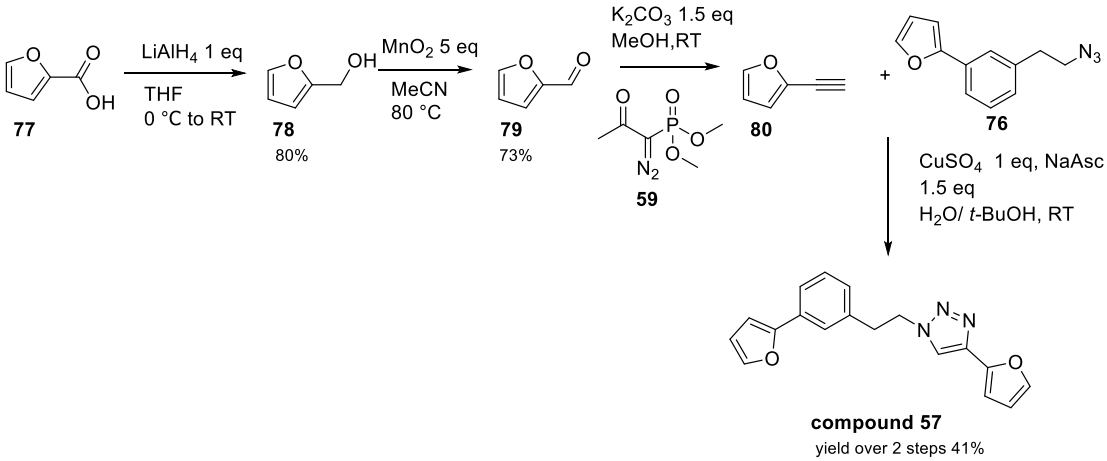

*Scheme 18 The synthetic route for compound **57***

3. Conclusion and future work

3.1 Conclusion

Overall, four new lead compounds were synthesised. For the synthesis of compounds **56** and **57**, two synthetic routes were designed. However, the first synthetic route led to inseparable by-products. The second synthetic route can avoid this. In addition, using the Stille coupling reaction to introduce the aromatic ring was more efficient, and the difficult to separate debrominated by-products can hence be avoided.

Due to the time restriction, the bioactivity data of these four compounds have not been gained.

3.2 Future work

3.2.1 Modify the terminal phenyl ring

The different substitutions can be introduced to the terminal benzene ring, like methoxy group, methyl group. Also, the different heterocycles still can be introduced, like pyridyl. The proposed synthetic route is similar to synthetic route 2. The Stille reagent can be synthesised through the reaction of aryl bromide and tributyltin chloride (Scheme 19).

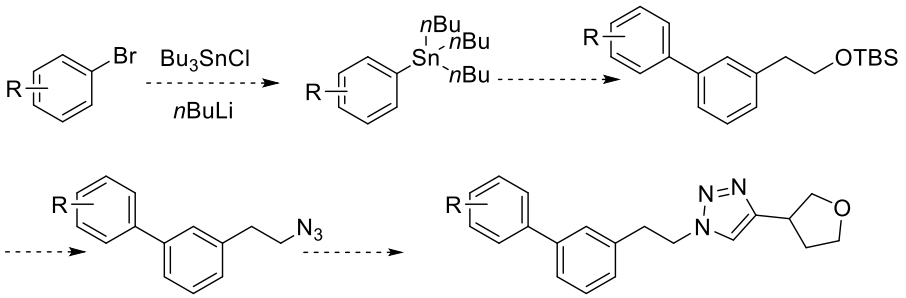

Scheme 19 Potential route to introduce different substitutions and heterocycles

3.2.2 Replacing the internal ring with heterocycles

The internal benzene ring also can be replaced with heterocycles, like furan, triazole, or

isoxazole. For example, the triazole ring can be introduced through the copper-catalyzed cycloaddition reaction. (Scheme 20)

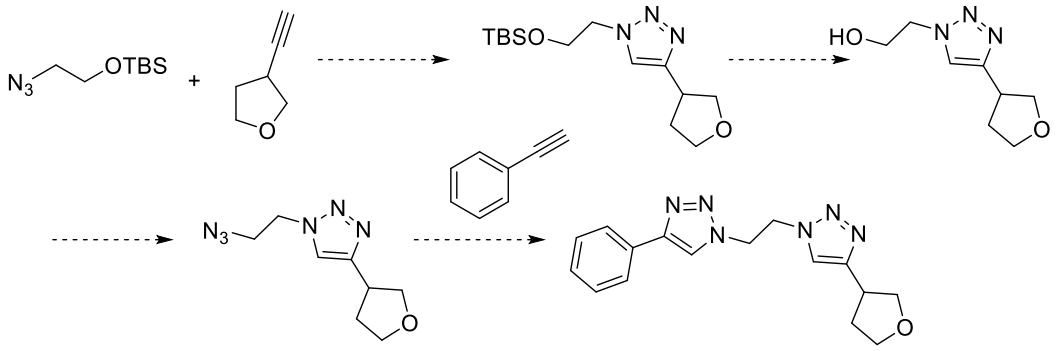

Scheme 20 Potential route to introduce second triazole ring

3.2.3 Replacing the aliphatic linker

The 2-carbon aliphatic linker can be replaced with an amide bond to improve the compound solubility. The first step is introducing the benzene ring through Stille coupling reaction. The amide bond will be introduced by copper-catalyzed reaction of aldehyde and trimethylsilyl azide, with *tert*-butyl peroxybenzoate (TBPB) acting as the oxidant and initiator.[44] The triazole will be introduced through a copper-catalyzed cycloaddition reaction (Scheme 21).

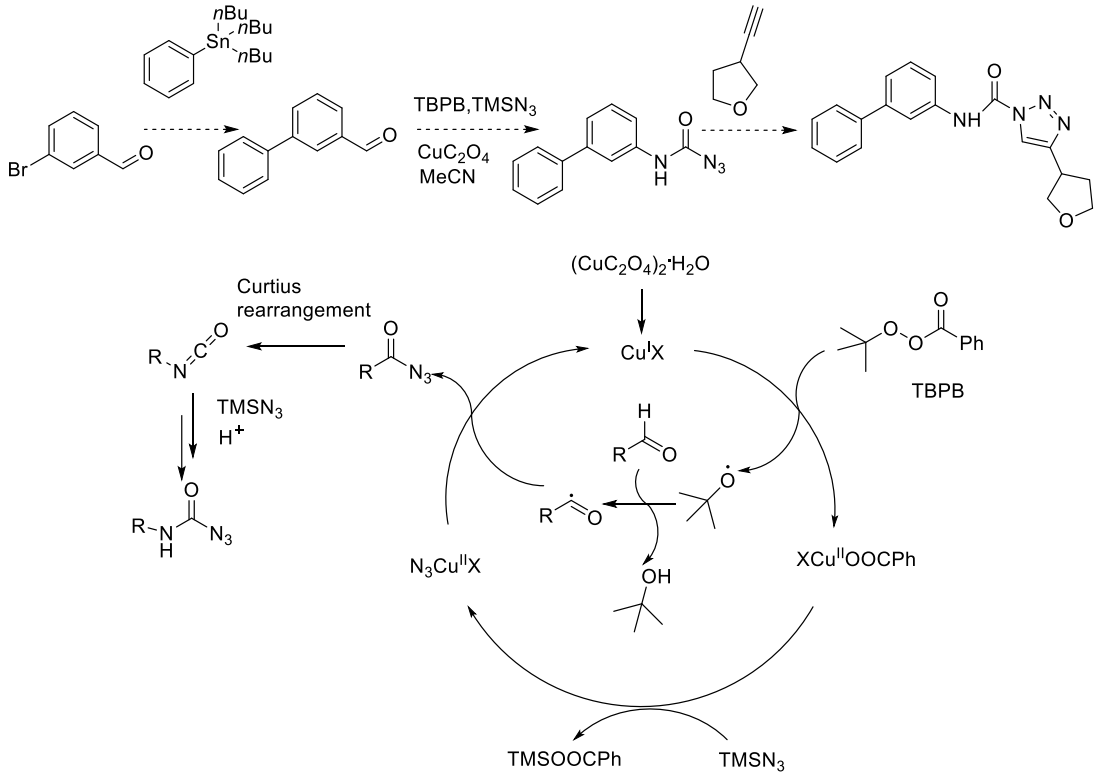

Scheme 21 Possible mechanism to introduce amide bond[44]

3.2.4 Separating the racemic mixture

Both compounds **55** and compound **56** are racemic. In the future, if the racemic compounds show good activity against trypanosomatid parasites, the racemic mixture could be separated using a chiral column to determine individual activities for both enantiomers.

3.2.5 Bioactivity testing

These four compounds will be sent to Professor Terry Smith group and test the bioactivity against *T.cruzi*, *T brucei* and *L. major.*

Experimental

4.1 General Procedures

All experiments were performed in oven-dried flasks (>80 °C) under a positive pressure of argon with magnetic stirring unless otherwise stated.

^{1}H NMR was recorded on a Bruker Avance 300 (300.1 MHz), Bruker Avance II 400 (400.1 MHz), and was referenced using deuterated solvents (chloroform-d 7.26 ppm). The chemical shifts are reported in parts per million (ppm) on the delta (δ) scale. The multiplicity of each signal is indicated by s (singlet), d (doublet), t (triplet), dd (doublet of doublets), dt (doublet of triplets), q (quartet) or m (multiplet). The coupling constants (*J*) are measure in Hertz (Hz) and the assigned proton in the spectra is given as H^{x}.

^{13}C NMR spectra were recorded on a Bruker Avance II 400 (101 MHz) and Bruker Avance III 500 (126MHz) instruments at room temperature and internal deuterium lock. The chemical shifts are reported in ppm on the δ scale and referenced using deuterated chloroform to 77.16 ppm.

Infrared (IR) spectra were recorded on a Shimadzu IR affinity-1 FTIR spectrometer using attenuated total reflectance (ATR) as the sampling technique. Absorption maxima are reported in wavenumbers (cm^{-1}). Only characteristic IR signals were selected and provided for each compound.

High-Resolution Mass Spectroscopy (HRMS) were recorded by the University of St Andrews Mass Spectrometry facility using NSI (nano-electrospray ionization). The parent ion is assigned.

Analytical Thin Layer Chromatography (TLC) was carried out on pre-coated (25 µm) Merck Kieselgel 60 F254 plates with visualisation by ultraviolet (UV) at 254 nm, and/or after stained with either a solution of 20% ceric ammonium molybdate w/v in H_2O or 20% potassium permanganate w/v in H_2O.

Flash Column Chromatography was carried out on Merck silica gel 60 (40–63 µm) under a positive pressure of compressed air. Reagent grade solvents were used as purchased.

Dry solvents were obtained through the following procedures:

DCM (CH_2Cl_2), toluene and tetrahydrofuran (THF) were obtained from the passage of two

columns of alumina through an MBRAUN (SPS-800) solvent purification system. Dimethylformamide (DMF) was obtained through distillation using 4 Å molecular sieves under atmospheric pressure and reserved with 4 Å molecular sieves under argon. All other reagents were used as purchased from Sigma Aldrich UK, Acros Organics UK, Fluorochem UK, Tokyo Chemical Industry Europe and Alfa Aesar UK and used as obtained unless stated otherwise. “Brine” refers to a saturated aqueous solution of sodium chloride (NaCl) in deionized water.

Reactions carried out at -78 °C were prepared using a mixture of acetone and dry ice.

4.2 Experimental details

Tetrahydrofuran-3-carbaldehyde 57

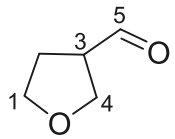

DMSO (200 mg, 2.2 mmol) was added to a solution of oxalyl chloride (150 mg, 1.2 mmol) in dry DCM (0.2 M) at -78 °C, then followed by tetrahydro-3-furan MeOH (100 mg, 1.0 mmol). After stirring for 1 hour at -78 °C, the triethylamine (500 mg, 5.0 mmol) was added dropwise. The reaction mixture was stirred 30 minutes at RT and then quenched with aq.NH_4Cl, extracted with DCM, dried over Na_2SO_4, filtered, and concentrated under reduced pressure at 0 °C, affording 150 mg crude product. The product was carried to the next step without further purification.

R_f 0.50 (40% EtOAc/Hexane); **^{1}H NMR** (500 MHz, $CDCl_3$) δ 9.66 (1H, d, *J* = 2.4 Hz, H^5), 4.10 (1H, m, H^4), 3.92 – 3.85 (2H, m, H^1), 3.79 – 3.73 (1H, m, H^4), 3.10 – 3.02 (m, 1H, H^3), 2.25 – 2.10 (2H, m, H^2).

Data is in accordance with the literature.[45]

Ohira Bestmann Regent 59

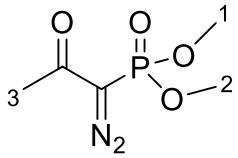

NaH (60 % dispersion in mineral oil) (1800 mg, 44.0 mmol) was added to the solution of dimethyl-2-oxopropyl phosphonate (6000 mg, 36.0 mmol) in toluene (12 mL) at 0 °C. After stirring for 1 h, a solution of 4-acetamidobenzensulfonyl (7800 mg, 32.4 mmol) in THF (10 mL) was added dropwise. The reaction was stirred overnight at RT and then petroleum ether (20 mL) was added. The precipitate was filtered off and washed 3 times with diethyl ether. The reaction mixture was concentrated under reduced pressure and purification by column chromatography (Solvent 90% EtOAc/Hexane) afforded **59** (3400 mg, 51 %) as a yellow oil.

R_f 0.33 (90% EtOAc/Hexane); **^{1}H NMR** (400 MHz, $CDCl_3$) δ 3.81 (6H, d, *J* = 11.9 Hz, $H^{1,2}$), 2.23

(3H, s, H^3).

Data is in accordance with the literature.[46]

3-Ethynyltetrahydrofuran 60

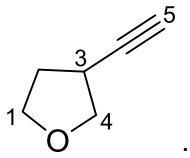

.

Ohira-Bestmann reagent (100 mg, 0.5 mmol) was added to the solution of Tetrahydrofuran-3-carbaldehyde **55** (50 mg, 0.5 mmol), potassium carbonate (110 mg, 0.8 mmol) in MeOH (5 mL) and then the reaction mixture was stirred 2 h at RT. The mixture was diluted with pentane/ ether 1:1 (5 mL: 5 mL), quenched with water, washed with brine, dried over Na_2SO_4 and concentrated under reduced pressure at 0 °C, affording crude product 45 mg. The product was carried to the next step without further purification.

R_f 0.16 (40 EtOAc/Hexane); **^{1}H NMR** (400 MHz, $CDCl_3$) δ 4.01 (1H, dd, *J* = 8.2, 7.3 Hz, H^4), 3.95 – 3.80 (2H, m, H^1), 3.66 (1H, dd, *J* = 8.2, 7.0 Hz, H^4), 3.03 – 2.91 (1H, m, H^3), 2.27 – 2.18 (1H, m, H^2), 2.09 (1H, d, *J* = 2.4 Hz, H^5), 2.05 – 1.95 (1H, m, H^2).

Data is in accordance with the literature.[47]

1-(2-azidoethyl)-3-bromobenzene 62

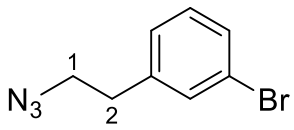

The triethylamine (380 mg, 3.8 mmol) and methanesulfonyl chloride (340 mg, 3 mmol) was added to the solution of 2-(3-bromophenyl)ethanol (500 mg, 2.5 mmol) in 5 mL DCM at 0 °C. The reaction was stirred for 1h at 0 °C, then the water was added to quench the reaction. The mixture was extracted by EtOAc, dried over Na_2SO_4, and concentrated under reduced pressure. The crude material was then dissolved in DMF (5 mL) and sodium azide (330 mg, 5.0 mmol) was added. The reaction mixture was heated to 85 °C and stirred for 17h. After the reaction finishing, the reaction mixture was concentrated, and then water was added.

The organics were extracted with DCM, dried over Na_2SO_4, and concentrated under reduced pressure. Purification by column chromatography (Solvent 20% EtOAc/Hexane) afforded **62** (300 mg, 81 %) as a colourless oil.

R_f 0.63 (20% EtOAc/Hexane); **^{1}H NMR** (500 MHz, $CDCl_3$) δ 7.39 (2H, m, ArH), 7.23 – 7.12 (2H, m, ArH), 3.51 (2H, t, *J* = 7.2 Hz, H^1), 2.86 (2H, t, *J* = 7.2 Hz, H^2).

Data is in accordance with the literature.[48]

1-(3-bromophenethyl)-4-(tetrahydrofuran-3-yl)-1H-1,2,3-triazole 63

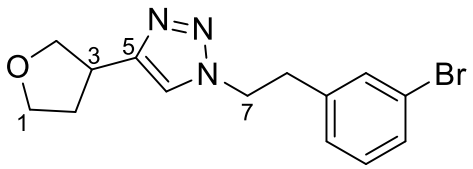

The azide **62** (200 mg, 2.0 mmol), alkyne **60** (500 mg, 2.2 mmol), $CuSO_4{\cdot}5H_2O$ (500 mg, 2.0 mmol) and sodium ascorbate (600 mg, 3.0 mmol) were added to the water/ *tert*-butanol (1:1) (0.5 mL: 0.5 mL) solution and then stirred for 48h at RT. The reaction was quenched with water and then filtered. The organics were extracted with DCM, dried over Na_2SO_4, and concentrated under reduced pressure. Purification by column chromatography (Solvent 90% EtOAc/Hexane) afforded **63** (400 mg, 59 %) as a white solid.

R_f 0.33 (100% EtOAc); **Mp.** 66-67 °C; **IR**(ATR) 3109(C-H), 1589(C=C), 1049(C-O), 682(C-Br) cm^{-1}; **^{1}H NMR** (500 MHz, $CDCl_3$) δ 7.38 (1H, ddd, *J* = 8.1, 2.0, 1.0 Hz, ArH), 7.21 – 7.13 (2H, m, ArH), 7.05 (1H, s, H^6), 6.99 (1H, dd, *J* = 7.7, 1.4 Hz, ArH), 4.53 (2H, td, *J* = 7.1, 1.8 Hz, H^7), 4.09 (1H, dd, *J* = 8.4, 7.0 Hz, H^4), 3.96 – 3.86 (2H, m, H^1), 3.73 (1H, dd, *J* = 8.4, 6.3 Hz, H^4), 3.61 – 3.53 (1H, m, H^3), 3.17 (2H, t, *J* = 7.1 Hz, H^8), 2.34 (1H , dtd, *J* = 12.4, 7.9, 5.8 Hz, H^2), 2.04 (1H, ddt, *J* = 12.6, 8.0, 6.7 Hz, H^2); **^{13}C NMR** (500 MHz, $CDCl_3$) δ 149.61 (C(quat), C^5), 139.75 (C(quat), ArC), 132.18 (CH, ArC), 130.67 (CH, ArC), 130.62(CH, ArC), 127.74 (CH, ArC), 123.13 (C(quat), ArC), 121.04 (CH, C^6), 73.72 (CH_2, C^4), 68.27 (CH_2, C^1), 51.69 (CH_2, C^7), 36.82 (CH_2, C^8), 36.78 (CH, C^3), 33.37 (CH_2, C^2); **HRMS** (ESI^+) Calc. for $C_{14}H_{16}BrN_3O$ [M+Na^+] 322.0550 (^{35}Br) and 324.0530 (^{37}Br), found 322.0546 and 324.0525.

(3-bromophenethoxy)(tert-butyl)dimethylsilane 70

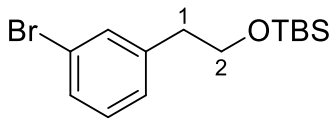

The imidazole(660 mg, 10.0 mmol) and *tert*-butyldimethylsilyl chloride (750 mg, 5.0 mmol) was added to the solution of 2-(3-bromophenyl)ethanol(0.4 mL, 2.0 mmol) in DCM (13 mL) at RT, and then was stirred for 1.5 h. Then the organics were diluted with DCM, washed with aq.$NaHCO_3$, brine, and dried over Na_2SO_4, and then concentrated under reduced pressure to yield the compound **70** (776 mg, 99 %) as a colourless oil.

R_f 0.6 (100% Hexane); **^{1}H NMR** (400 MHz, Chloroform-*d*) δ 7.37 (1H, dd, *J* = 1.6, 0.6 Hz, ArH), 7.33 (1H, dt, *J* = 6.7, 2.3 Hz, ArH), 7.17 – 7.11 (2H, m, ArH), 3.79 (2H, t, *J* = 6.8 Hz, H^2), 2.78 (2H, t, *J* = 6.7 Hz, H^1), 0.86 (9H, s, $SiC(CH_3)_3$), -0.03 (6H, s,2x$SiCH_3$).

Data is in accordance with the literature.[48]

tert-butyl(2-(2',3'-dichloro-[1,1'-biphenyl]-3-yl)ethoxy)dimethylsilane 68

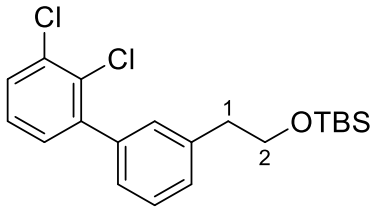

Compound **70** (600 mg, 2.0 mmol), 2,3-dichlorophenylboric acid (432 mg, 2.4 mmol), and sodium carbonate (600 mg, 2.0 mmol) were dissolved in the mixture of ethanol: water: toluene (3:1:1, 5 mL). The mixture was degassed 10 mins under nitrogen, and then tetrakis(triphenylphosphine) Palladium (114 mg, 0.1 mmol) was added and the reaction mixture was heated in a sealed tube at 100 °C for 24 h. The reaction was quenched with aq.$NaHCO_3$, extracted with DCM, washed with brine, dried over Na_2SO_4 and concentrated under reduced pressure. Purification by column chromatography (Solvent 2% EtOAc/Hexane) afforded compound **68** (360 mg, 51 %) as a colourless oil. (Column twice to get rid of by-product, the by-product is less polar than the product)

R_f 0.27 (2% EtOAc/Hexane); **IR**(ATR) 2943(C-H),1741(C=C), 1097(C-O),833(C-Cl) cm^{-1}; **^{1}H NMR**

(500 MHz, DMSO-d_6) δ 7.66 (1H, dd, *J* = 8.0, 1.6 Hz, ArH), 7.43 (1H, t, *J* = 7.9 Hz, ArH), 7.38 (1H, td, *J* = 7.5, 0.9 Hz, ArH), 7.33 (1H, dd, *J* = 7.7, 1.6 Hz, ArH), 7.29 – 7.24 (3H, m, ArH), 3.81 (2H, t, *J* = 6.6 Hz, H^2), 2.80 (2H, t, *J* = 6.5 Hz, H^1), 0.80 (9H, s, $SiC(CH_3)_3$), -0.07 (6H, s, $2xSiCH_3$); **^{13}C NMR** (126 MHz, DMSO) δ 142.53(C(quat), ArC), 139.33(C(quat), ArC), 138.39(C(quat), ArC), 132.29(C(quat), ArC), 130.04(CH, ArC), 129.86(CH, ArC), 129.63(CH, ArC), 128.89(CH, ArC), 128.29(CH, ArC), 128.00(CH, ArC), 126.81(CH, ArC), 63.69(CH_2, C^2), 38.64(CH_2, C^1), 25.78($3xCH_3$, $SiC(CH_3)_3$), 17.93(C(quat), $SiC(CH_3)_3$), -5.43($2xCH_3$, $SiCH_3$); **HRMS** (ESI^+) Calc. for $C_{20}H_{26}Cl_2Osi$ (^{35}Cl) [M+Na^+] 403.1200, found 403.1009.

2-(3-bromophenethoxy)tetrahydro-2H-pyran 77

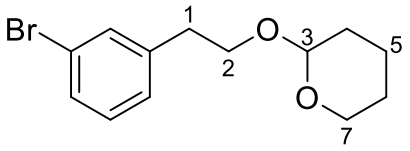

The dihydropyran(0.4 mL, 3.7 mmol)and pyridium toluene-4-sulfonate(3 mg, 0.01 mmol) was added into the solution of 2-(3-bromophenyl)ethanol (0.068 mL, 0.5 mmol) in DCM (3 mL) at RT, and then was stirred for 24h. The reaction was quenched with aq.$NaHCO_3$, extracted with DCM, washed with brine, dried over Na_2SO_4, and concentrated under reduced pressure. Purification by column chromatography (Solvent 10% EtOAc/Hexane) afforded compound **77** (490 mg, 99 %) as a colourless oil.

R_f 0.36 (10% EtOAc/Hexane); **^{1}H NMR** (400 MHz, Chloroform-*d*) δ 7.41 (1H, ddt, *J* = 2.2, 1.5, 0.6 Hz, ArH), 7.34 (1H, dt, *J* = 6.7, 2.1 Hz, ArH), 7.19 – 7.12 (2H, m, ArH), 4.59 (1H, dd, *J* = 4.2, 2.8 Hz, H^3), 3.93 (1H, dt, *J* = 9.7, 7.1 Hz, H^2), 3.72 (1H, ddd, *J* = 11.4, 8.5, 3.4 Hz, H^7), 3.62 – 3.56 (1H, m, H^2), 3.53 – 3.37 (1H, m, H^7), 2.88 (2H, t, *J* = 7.0 Hz, H^1), 1.98 – 1.38 (6H, m, H^4,H^5,H^6).

Data is in accordance with the literature.[49]

2-(2-(2',3'-dichloro-[1,1'-biphenyl]-3-yl)ethoxy)tetrahydro-2H-pyran 78

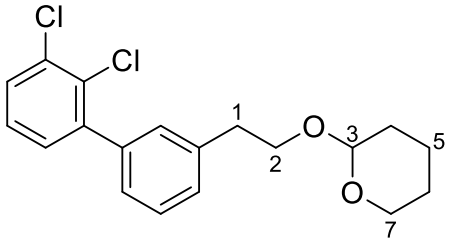

Compound **77** (200 mg, 0.7mmol), 2,3-dichlorophenylboric acid (160 mg, 0.9 mmol), and sodium carbonate (223 mg, 2.1mmol) were dissolved in the mixture of ethanol: water: toluene (3:1:1, 5 mL). The mixture was degassed 10 mins under nitrogen, and then tetrakis(triphenylphosphine) Palladium (40 mg, 0.05 mmol) was added and the reaction mixture was heated in a sealed tube at 100 °C for 24 h. The reaction was quenched with sodium bicarbonate, extracted with DCM, washed with brine, dried over Na_2SO_4, and then concentrated under reduced pressure. Purification by column chromatography (Solvent 5% EtOAc/Hexane) afforded compound **78** (50 mg, 20 %) as a colourless oil. (Column twice to get rid of by-product, the by-product is less polar than the product)

R_f 0.15 (5% EtOAc/Hexane); **IR**(ATR) 2939(C-H),1612(C=C),1031(C-O),773(C-Cl)cm^{-1}; **^{1}H NMR** (500 MHz, DMSO-d_6) δ 7.66 (1H, dd, *J* = 8.0, 1.6 Hz, ArH), 7.43 (1H, t, *J* = 7.8 Hz, ArH), 7.39 (1H, td, *J* = 7.6, 0.7 Hz, ArH), 7.35 (1H, dd, *J* = 7.7, 1.6 Hz, ArH), 7.32 – 7.29 (2H, m, ArH), 7.25 (1H, dt, *J* = 7.6, 1.5 Hz, ArH), 4.58 (1H, t, *J* = 3.6 Hz, H^3), 3.84 (1H, dt, *J* = 9.7, 7.0 Hz, H^2), 3.66 – 3.55 (2H, m, H^2,H^7), 3.38 – 3.34 (1H, m, H^7), 2.89 (2H, t, *J* = 6.8 Hz, H^1), 1.74 – 1.27 (6H, m, H^4,H^5,H^6); **^{13}C NMR** (126 MHz, DMSO) δ 142.51(C(quat), ArC), 139.38(C(quat), ArC), 138.46(C(quat), ArC), 132.29(C(quat), ArC), 130.08(CH, ArC), 129.66(2xCH, ArC), 128.66(CH, ArC), 128.32(CH, ArC), 128.15(CH, ArC), 126.83(CH, ArC), 97.67(CH, C^3), 67.24(CH_2, C^2), 61.09(CH_2, C^7), 35.46(CH_2, C^1), 30.24(CH_2, C^4), 25.05(CH_2, C^6), 19.03(CH_2, C^5); **HRMS** (ESI^+) Calc. for $C_{19}H_{20}Cl_2O_2$ (^{35}Cl) [M+Na^+] 373.0733, found 373.0720.

2-(2',3'-dichloro-[1,1'-biphenyl]-3-yl)ethanol 66

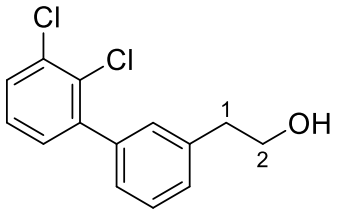

The tetrabutylammonium fluoride(482 mg, 1.8 mmol) was added to the solution of compound **68** (350 mg, 0.9 mmol) in THF at 0 °C, then was stirred for 2 h. The reaction was quenched with water, extracted with EtOAc, washed with brine, dried over Na_2SO_4, and then concentrated under reduced pressure. Purification by column chromatography (Solvent 40% EtOAc/Hexane) afforded compound **66** (196 mg,80 %) as a colourless oil.

R_f 0.31 (40% EtOAc/Hexane); **IR**(ATR) 3331(O-H),2943(C-H), 1585(C=C),1039(C-O),781(C-Cl)cm^{-1}; **^{1}H NMR** (500 MHz, DMSO-d_6) δ 7.66 (1H, dd, *J* = 8.0, 1.6 Hz, ArH), 7.43 (1H, t, *J* = 7.8 Hz, ArH), 7.40 – 7.35 (2H, m, ArH), 7.29 – 7.24 (3H, m, ArH), 4.67 (1H, t, *J* = 5.2 Hz, OH), 3.64 (2H, td, *J* = 7.0, 5.1 Hz, H^2), 2.78 (2H, t, *J* = 7.0 Hz, H^1); **^{13}C NMR** (126 MHz, DMSO) δ 142.51(C(quat), ArC), 139.75(C(quat), ArC), 138.39(C(quat), ArC), 132.31(C(quat), ArC), 130.15(CH, ArC), 129.64(2xCH, ArC), 128.71(CH, ArC), 128.33(CH, ArC), 128.07(CH, ArC), 126.68(CH, ArC), 62.01(CH_2, C^2), 38.87(CH_2, C^1); **HRMS** (ESI^+) Calc. for $C_{14}H_{12}Cl_2O$ (^{35}Cl) [$M+Na^+$] 289.0157, found 289.0150.

3'-(2-azidoethyl)-2,3-dichloro-1,1'-biphenyl 69

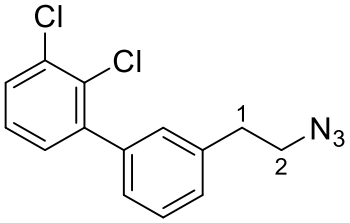

The iodine (120 mg, 0.9 mmol) and triphenylphosphine(240 mg, 0.9 mmol) was added to the dry acetonitrile (2 mL) and stirred for 15 mins, and then the compound **66** (120 mg, 0.45 mmol) was added and reacted 12h at RT. The reaction was quenched with sodium sulfite, extracted with EtOAc, washed with brine, dried over Na_2SO_4, and then concentrated under reduced pressure. The crude material was then dissolved in DMF (3 mL), and sodium azide (280 mg, 0.9 mmol) was added. The reaction mixture was heated to 85 °C and stirred for 6 h.

After the reaction finishing, the reaction mixture was concentrated, and then water was added. The organics were extracted with DCM, dried over Na_2SO_4, and concentrated under reduced pressure. Purification by column chromatography (Solvent 5% EtOAc/Hexane) afforded **69** (67 mg, 51 %) as a colourless oil.

R_f 0.2 (5% EtOAc/Hexane); **IR**(ATR) 2943(C-H),2092(N=N=N),1583(C=C),781(C-Cl)cm^{-1}; **^{1}H NMR** (500 MHz, DMSO-d_6) δ 7.67 (1H, dq, *J* = 8.0, 1.6 Hz, ArH), 7.43 (2H, ddd, *J* = 14.7, 7.9, 3.9 Hz, ArH), 7.39 – 7.33 (3H, m, ArH), 7.30 (1H, dt, *J* = 7.6, 1.6 Hz, ArH), 3.61 (2H, td, *J* = 7.1, 2.3 Hz, H^2), 2.92 (2H, td, *J* = 7.1, 2.3 Hz, H^1); **^{13}C NMR** (126 MHz, DMSO) δ 142.33(C(quat), ArC), 138.66(C(quat), ArC), 138.55(C(quat), ArC), 132.33(C(quat), ArC), 130.13(CH, ArC), 129.73(CH, ArC), 129.62(CH, ArC), 128.65(CH, ArC), 128.38(CH, ArC), 128.35(CH, ArC), 127.29(CH, ArC), 51.42(CH_2, C^2), 34.34(CH_2, C^1); **HRMS** (ESI^+) Calc. for $C_{14}H_{11}Cl_2N_3$ (^{35}Cl) [M+Na^+] 314.0222, found 314.0217.

1-(2-(2',3'-dichloro-[1,1'-biphenyl]-3-yl)ethyl)-4-(tetrahydrofuran-3-yl)-1H-1,2,3-triazole 55

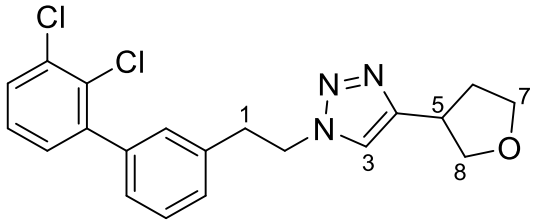

The azide **69** (87 mg, 0.2 mmol), alkyne **60** (20 mg, 0.2 mmol), $CuSO_4{\cdot}5H_2O$ (50 mg, 0.2 mmol) and sodium ascorbate (60 mg, 0.3 mmol) were added to the water/ *tert*-butanol (1:1) (0.5 mL:0.5 mL)solution and then stirred for 5 h at RT. The reaction was quenched with water and then filtered. The organics were extracted with DCM, dried over Na_2SO_4, and concentrated under reduced pressure. Purification by column chromatography (Solvent 90% EtOAc/Hexane) afforded **55** (31 mg, 38 %) as a colourless oil.

R_f 0.37 (100% EtOAc); **IR**(ATR) 2947(C-H), 1585(C=C),1049(C-O),782(C-Cl)cm^{-1}; **^{1}H NMR** (500 MHz, Chloroform-*d*) δ 7.47 (1H, dd, *J* = 8.0, 1.6 Hz, ArH), 7.37 (1H, t, *J* = 7.6 Hz, ArH), 7.29 (1H, dt, *J* = 7.7, 1.5 Hz, ArH), 7.24 (1H, d, *J* = 7.9 Hz, ArH), 7.16 (1H, dd, *J* = 7.6, 1.6 Hz, ArH), 7.13 (1H, dt, *J* = 7.6, 1.5 Hz, ArH), 7.09 (1H, d, *J* = 1.8 Hz, ArH), 7.07 (1H, s, H^3), 4.59 (2H, t, *J* = 7.2

Hz, H^2), 4.07 (1H, dd, *J* = 8.4, 7.1 Hz, H^8), 3.97 – 3.84 (2H, m, H^7), 3.70 (1H, dd, *J* = 8.4, 6.5 Hz, H^8), 3.55 (1H, dq, *J* = 8.3, 6.7 Hz, H^5), 3.25 (2H, t, *J* = 7.2 Hz, H^1), 2.31 (1H, dtd, *J* = 12.3, 7.9, 5.8 Hz, H^6), 2.00 (1H, ddt, *J* = 12.3, 8.0, 6.8 Hz, H^6); **^{13}C NMR** (126 MHz, $CDCl_3$) δ 149.21(C(quat), C^4), 142.44(C(quat), ArC), 139.90(C(quat), ArC), 137.20(C(quat), ArC), 133.77(C(quat), ArC), 131.11(C(quat), ArC), 129.76(CH, ArC), 129.74(CH, ArC), 129.47(CH, ArC), 128.77(CH, ArC), 128.42(CH, ArC), 128.18(CH, ArC), 127.37(CH, ArC), 120.78(CH, C^3), 73.43(CH_2, C^8), 68.04(CH_2, C^7), 51.66(CH_2, C^2), 36.87(CH_2, C^1), 36.51(CH, C^5), 33.06(CH_2, C^6); **HRMS** (ESI^+) Calc. for $C_{20}H_{19}Cl_2N_3O$ (^{35}Cl) [M+Na^+] 410.0797, found 410.0787.

tert-butyl(3-(furan-2-yl)phenethoxy)dimethylsilane 73

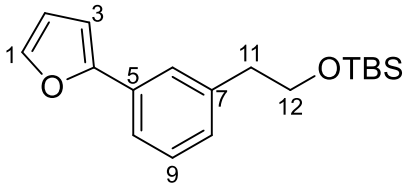

The 2-(tributylstannyl) furan (0.6 mL, 1.9 mmol) and tetrakis(triphenylphosphine)Palladium (110 mg, 0.2 mmol) was added to the solution of compound **70** (500 mg, 1.6 mmol) in dioxane (2 mL). Then the solution was heated to 101 °C and stirred for 36 h. The cooled mixture was quenched with saturated KF solution and then filtered through celite. The organic layer was separated, washed with brine, dried over Na_2SO_4, and concentrated under reduced pressure. Purification by column chromatography (Solvent 3% EtOAc/Hexane) afforded **73** (300 mg, 63%) as a yellow oil.

R_f 0.3 (3% EtOAc/Hexane); **IR**(ATR) 2931(C-H), 1465(C=C),1093(C-O) cm^{-1}; **^{1}H NMR** (500 MHz, Chloroform-*d*) δ 7.52 (2H, dt, *J* = 9.3, 1.7 Hz, ArH), 7.46 (1H, dd, *J* = 1.8, 0.8 Hz, H^1), 7.29 (1H, t, *J* = 7.6 Hz, ArH), 7.11 (1H, dt, *J* = 7.6, 1.5 Hz, ArH), 6.63 (1H, dd, *J* = 3.3, 0.8 Hz, ArH), 6.47 (1H, dd, *J* = 3.4, 1.8 Hz, ArH), 3.83 (2H, t, *J* = 7.0 Hz, H^{12}), 2.85 (2H ,t, *J* = 7.0 Hz,H^{11}), 0.87 (9H ,s, $SiC(CH_3)_3$), -0.01 (6H,s,2x$SiCH_3$); **^{13}C NMR** (126 MHz, $CDCl_3$) δ 154.24(C(quat), C^4), 142.06(CH, C^1), 139.81(C(quat), ArC), 130.91(C(quat), ArC), 128.68(CH, ArC), 128.41(CH, ArC), 124.74(CH, ArC), 121.84(CH, ArC), 111.73(CH, ArC), 104.97(CH, ArC), 64.56(CH_2, C^{12}), 39.74(CH_2, C^{11}), 26.06(3xCH_3, $SiC(CH_3)_3$), 18.47(C(quat), $SiC(CH_3)_3$), -5.27(2xCH_3, $SiCH_3$); **HRMS** (ESI^+) Calc. for $C_{18}H_{26}O_2Si$ [M+Na^+] 325.1594, found 325.1587.

2-(3-(furan-2-yl)phenyl)ethan-1-ol 75

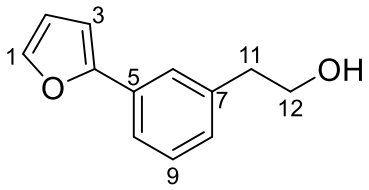

The tetrabutylammonium fluoride(484 mg, 1.8 mmol) was added to the solution of compound **73** (280 mg, 0.9 mmol) in THF (2 mL) at 0 °C, then was stirred for 2 h. The reaction was quenched with water, extracted with EtOAc, washed with brine, dried over Na_2SO_4, and then concentrated under reduced pressure. Purification by column chromatography (Solvent 40% EtOAc/Hexane) afforded compound **75** (140 mg, 80 %) as sticky yellow oil.

R_f 0.25 (40% EtOAc/Hexane); **IR**(ATR) 3360(O-H), 2942(C-H), 1608(C=C), 1043(C-O) cm^{-1}; **^{1}H NMR** (500 MHz, Chloroform-*d*) δ 7.55 (2H, dd, *J* = 6.8, 1.4 Hz, ArH), 7.47 (1H, dd, *J* = 1.8, 0.7 Hz, H^1), 7.38 – 7.31 (1H, m, ArH), 7.14 (1H, dt, *J* = 6.5, 1.1 Hz, ArH), 6.66 (1H, dd, *J* = 3.3, 0.8 Hz, ArH), 6.47 (1H, dd, *J* = 3.3, 1.8 Hz, ArH), 3.91 (2H, t, *J* = 6.5 Hz, H^{12}), 2.91 (2H, t, *J* = 6.5 Hz, H^{11}), 1.50 (1H, br, OH); **^{13}C NMR** (126 MHz, $CDCl_3$) δ 154.30(C(quat), C^4), 142.48(CH, C^1), 139.33(C(quat), ArC), 131.57(C(quat), ArC), 129.36(CH, ArC), 128.44(CH, ArC), 124.76(CH, ArC), 122.47(CH, ArC), 112.05(CH, ArC), 105.51(CH, ArC), 64.03 (CH_2, C^{12}), 31.36(CH_2, C^{11}); **HRMS** (ESI^+) Calc. for $C_{12}H_{12}O_2$ [$M+H^+$] 189.0910, found 189.0907.

2-(3-(2-azidoethyl)phenyl)furan 76

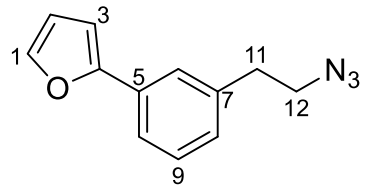

The iodine (140 mg, 1.1 mmol) and triphenylphosphine(280 mg, 1.1 mmol) was added to the dry acetonitrile and stirred for 15 mins, and then the compound **75** (100 mg, 0.5 mmol) was added and reacted 12h at RT. The reaction was quenched with water, extracted with EtOAc, washed with brine, dried over Na_2SO_4, and then concentrated under reduced pressure. The crude material was then dissolved in 3 mL DMF, and sodium azide (309 mg, 1.1 mmol) was

added. The reaction mixture was heated to 85 °C and stirred for 6 h. After the reaction finishing, the reaction mixture was concentrated, and then water was added. The organics were extracted with DCM, dried over Na_2SO_4, and concentrated under reduced pressure. Purification by column chromatography (Solvent 2% EtOAc/Hexane) afforded **76** (62 mg, 54 %) as sticky yellow oil.

R_f 0.28 (2% EtOAc/Hexane); **IR**(ATR) 2927(C-H), 2092(N=N=N), 1608(C=C), 1008(C-O); **^{1}H NMR** (500 MHz, Chloroform-*d*) δ 7.59 – 7.50 (2H, m, ArH), 7.47 (1H, dd, *J* = 1.8, 0.8 Hz, H^1), 7.34 (1H,t, *J* = 7.7 Hz, ArH), 7.12 (1H, dt, *J* = 7.6, 1.3 Hz, ArH), 6.66 (1H, dd, *J* = 3.3, 0.8 Hz, ArH), 6.48 (1H, dd, *J* = 3.3, 1.8 Hz, ArH), 3.54 (2H, t, *J* = 7.3 Hz, H^{12}), 2.93 (2H, t, *J* = 7.3 Hz, H^{11}); **^{13}C NMR** (126 MHz, $CDCl_3$) δ 154.22(C(quat), C^4), 142.27(CH, C^1), 138.62(C(quat), ArC), 131.37(C(quat), ArC), 129.15(CH, ArC), 127.88(CH, ArC), 124.23(CH, ArC), 122.47(CH, ArC), 111.82 (CH, ArC), 105.34(CH, ArC), 52.54(CH_2, C^{12}), 35.54(CH_2, C^{11}); **HRMS** (ESI^+) Calc. for $C_{12}H_{11}N_3O$ [M+H^+] 214.0975, found 214.0971.

1-(3-(furan-2-yl)phenethyl)-4-(tetrahydrofuran-3-yl)-1H-1,2,3-triazole 56

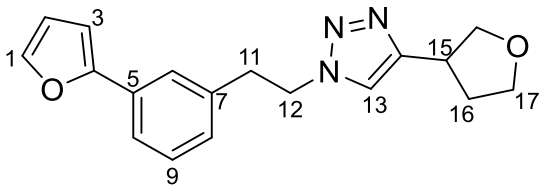

The azide **76** (53mg, 0.3 mmol), alkyne **60** (20 mg, 0.2 mmol), $CuSO_4{\cdot}5H_2O$ (60 mg, 0.3 mmol) and sodium ascorbate (80 mg, 0.6 mmol) were added to the water/ *tert*-butanol (1:1) solution and then stirred for 4 h at RT. The reaction was quenched with water and then filtered. The organics were extracted with DCM, dried over Na_2SO_4, and concentrated under reduced pressure. Purification by column chromatography (Solvent 90% EtOAc/Hexane) afforded **55** (20 mg, 40 %) as sticky yellow oil.

R_f 0.30 (100% EtOAc); **IR**(ATR) 2951(C-H), 1685(C=C),1159(C-O) cm^{-1}; **^{1}H NMR** (500 MHz, Chloroform-*d*) δ 7.55 (1H, dt, *J* = 8.0, 1.3 Hz, ArH), 7.46 (1H, dd, *J* = 1.8, 0.7 Hz, H^1), 7.35 (1H, d, *J* = 1.9 Hz, ArH), 7.30 (1H, t, *J* = 7.7 Hz, ArH), 7.03 (1H, d, *J* = 0.6 Hz, ArH), 6.97 (1H, dt, *J* = 7.7, 1.3 Hz, ArH), 6.62 (1H, dd, *J* = 3.4, 0.8 Hz, ArH), 6.47 (1H, dd, *J* = 3.4, 1.8 Hz, ArH), 4.58

(2H, td, *J* = 7.1, 2.4 Hz, H^{12}), 4.05 (1H, dd, *J* = 8.4, 7.1 Hz, H^{18}), 3.88 (2H, ddd, *J* = 7.5, 6.4, 4.8 Hz, H^{17}), 3.69 (1H, dd, *J* = 8.4, 6.5 Hz, H^{18}), 3.55 (1H, dd, *J* = 8.0, 6.5 Hz, H^{15}), 3.22 (2H, t, *J* = 7.2 Hz, H^{11}), 2.29 (1H, dtd, *J* = 12.6, 7.8, 6.0 Hz, H^{16}), 1.96 (1H, m, H^{16}); **^{13}C NMR** (126 MHz, $CDCl_3$) δ153.49(C(quat), C^4), 149.11(C(quat), ArCz), 142.38(CH_2, C^1), 137.74(C(quat), ArC), 131.48(C(quat), ArC), 129.31(CH, ArC), 127.74(CH, ArC), 124.17(CH, ArC), 122.70(CH, ArC), 120.86(CH_2, C^{13}), 111.87(CH, ArC), 105.50(CH_2, ArC), 73.43(CH_2, C^{18}), 68.00(CH_2, C^{17}), 51.75(CH_2, C^{12}), 37.07(CH_2, C^{11}), 36.53(CH, C^{15}), 33.09(CH_2, C^{16}); **HRMS** (ESI^+) Calc. for $C_{18}H_{19}N_3O_2$ [$M+H^+$] 310.1550, found 310.1549.

furan-2-ylmethanol 78

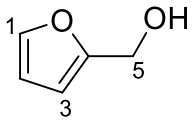

The 2-furoic acid (500 mg, 4.5 mmol) was added to the solution of LAH (170 mg, 4.5 mmol) in dry THF (5 mL) at 0 °C. Then the reaction was warmed to RT and stirred for 24 h. The reaction was washed with 10% KOH and extracted with DCM. The organic layer was then washed with 5% HCl, followed by brine, dried over Na_2SO_4, and concentrated under reduced pressure. Purification by column chromatography (Solvent 50% EtOAc/Hexane) afforded **55** (350 mg, 80 %) as a yellow oil.

R_f 0.56 (50% EtOAc/Hexane); **^{1}H NMR** (400 MHz, Chloroform-*d*) δ 7.41 (1H, dd, *J* = 1.9, 0.9 Hz, ArH), 6.35 (1H, dd, *J* = 3.2, 1.8 Hz, ArH), 6.30 (1H, dd, *J* = 3.3, 0.7 Hz, ArH), 4.62 (2H, s, H^5), 1.69 (1H, s, OH).

Data is in accordance with the literature.[50]

furan-2-carbaldehyde 79

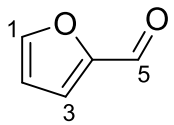

The MnO_2(88%, electrolytically precipitated) (443 mg, 5.0 mmol) was added to the solution of compound **78** (100 mg, 1.0 mmol) in MeCN (3 mL). Then, the reaction mixture was heated

to 80 °C for 4 h. The reaction mixture was filtered through celite and concentrated getting the yellow oil. Purification by column chromatography (Solvent 20% EtOAc/Hexane) afforded **79** (75 mg, 73 %) as a yellow oil.

R_f 0.34 (20% EtOAc/Hexane); **^{1}H NMR** (500 MHz, Chloroform-*d*) δ 9.67 (1H, d, *J* = 0.7 Hz, H^5), 7.70 (1H, dt, *J* = 1.6, 0.8 Hz, ArH), 7.28 (1H, dd, *J* = 3.6, 0.8 Hz, ArH), 6.61 (1H, dd, *J* = 3.6, 1.7 Hz, ArH).

Data is in accordance with the literature.[50]

2-ethynylfuran 80

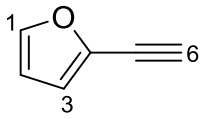

Ohira-Bestmann reagent (105 mg, 0.5 mmol) was added to the solution of compound **79** (50 mg, 0.5 mmol), potassium carbonate (108 mg, 0.8 mmol) in MeOH (2 mL) and then the reaction mixture was stirred 8 h at RT. The reaction mixture was diluted with pentane/ ether 1:1, quenched with water, washed with brine, dried over Na_2SO_4 and concentrated under reduced pressure at 20 °C. The product was carried to the next step without further purification.

R_f 0.81 (20% EtOAc/Hexane); **^{1}H NMR** (400 MHz, Chloroform-*d*) δ 7.39 (1H, dd, *J* = 1.9, 0.8 Hz, ArH), 6.67 – 6.64 (1H, m, ArH), 6.39 (1H, dd, *J* = 3.4, 1.9 Hz, ArH), 3.39 (1H, s, H^6).

Data is in accordance with the literature.[51]

4-(furan-2-yl)-1-(3-(furan-2-yl)phenethyl)-1H-1,2,3-triazole 57

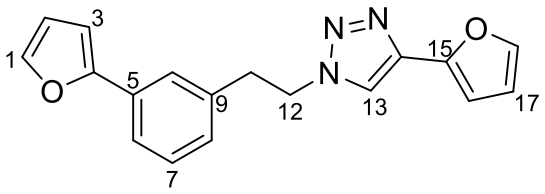

The azide **76** (115 mg, 0.5 mmol), $CuSO_4{\cdot}5H_2O$ (270 mg, 0.1 mmol) and sodium ascorbate (322 mg, 1.6 mmol) were added to the solution of alkyne **80** in water/ *tert*-butanol (1:1) and then stirred for 4 h at RT. The reaction was quenched with water and then filtered. The organics were extracted with DCM, dried over Na_2SO_4, and concentrated under reduced

pressure. Purification by column chromatography (Solvent 30% EtOAc/Hexane) afforded **55** (63 mg, 40 %) as a brown solid.

R_f 0.30 (30% EtOAc/Hexane); **Mp.** 114 °C; **IR**(ATR) 3109(C-H), 1475(C=C), 1002(C-O) cm^{-1}; **^{1}H NMR** (500 MHz, Chloroform-*d*) δ 7.56 (1H, dt, *J* = 7.8, 1.4 Hz, ArH), 7.51 (1H, s,H^{13}), 7.49 – 7.47 (1H, m, ArH), 7.46 (1H, dd, *J* = 1.9, 0.7 Hz, ArH), 7.42 (1H, dd, *J* = 1.8, 0.8 Hz, ArH), 7.31 (1H, t, *J* = 7.7 Hz, ArH), 7.00 (1H, dt, *J* = 7.7, 1.4 Hz, ArH), 6.80 (1H, dd, *J* = 3.4, 0.8 Hz, ArH), 6.64 (1H, dd, *J* = 3.4, 0.8 Hz, ArH), 6.47 (2H, ddd, *J* = 3.2, 1.8, 1.0 Hz, ArH), 4.66 (2H, t, *J* = 7.3 Hz, H^{12}), 3.28 (2H, t, *J* = 7.4 Hz, H^{11}); **^{13}C NMR** (126 MHz, $CDCl_3$) δ 153.59(C(quat), ArC), 146.36(C(quat), ArC), 142.37(CH, ArC), 142.12(CH, ArC), 140.44(C(quat), C^{14}), 137.47(C(quat), ArC), 131.58(C(quat), ArC), 129.38(CH, ArC), 127.79(CH, ArC), 124.05(CH, ArC), 122.80(CH, ArC), 119.65(CH, C^{13}), 111.86(CH, ArC), 111.56(CH, ArC), 106.63(CH, ArC), 105.53(CH, ArC), 51.77(CH_2, C^{12}), 36.92(CH_2, C^{11}); **HRMS** (ESI^+) Calc. for $C_{18}H_{15}N_3O_2$ [$M+H^+$] 306.1237, found 306.1228.

furan-3-ylmethanol 81

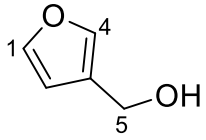

The 3-furoic acid (500 mg, 4.5 mmol) was added to the solution of LAH (170 mg, 4.5 mmol) in dry THF (5 mL) at 0 °C. Then the reaction was warmed to RT and stirred for 24 h. The organics were washed with 10% KOH and extracted with DCM. The organic layer was then washed with 5% HCl, followed by brine, dried over Na_2SO_4, and concentrated under reduced pressure. Purification by column chromatography (Solvent 50% EtOAc/Hexane) afforded **55** (340 mg, 78 %) as a yellow oil.

R_f 0.6 (50% EtOAc/Hexane); **^{1}H NMR** (500 MHz, Chloroform-*d*) δ 7.44 – 7.39 (2H, m, $H^{1,4}$), 6.44 (1H, dd, *J* = 1.8, 0.8 Hz, H^3), 4.57 (2H, s, H^5), 2.25 (1H, s, OH).

Data is in accordance with the literature.[50]

furan-3-carbaldehyde 82

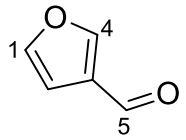

The MnO_2(88%, electrolytically precipitated) (443 mg, 5.0 mmol) was added to the solution of compound **81** (100 mg, 1.0 mmol) in MeCN (3 mL). Then, the reaction mixture was heated to 80 °C for 4 h. The reaction mixture was filtered through celite and concentrated getting the yellow oil. Purification by column chromatography (Solvent 20% EtOAc/Hexane) afforded **82** (68 mg, 70 %) as a yellow oil.

R_f 0.45 (20% EtOAc/Hexane); **^{1}H NMR** (500 MHz, Chloroform-*d*) δ 9.95 (1H, s, H^5), 8.09 – 8.06 (1H, m, ArH), 7.50 – 7.48 (1H, m, ArH), 6.80 (1H, d, *J* = 1.9 Hz, ArH).

Data is in accordance with the literature.[50]

3-ethynylfuran 83

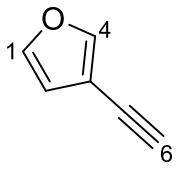

Ohira-Bestmann reagent (105 mg, 0.5 mmol) was added to the solution of compound **82** (50 mg, 0.5 mmol), potassium carbonate (108 mg, 0.8 mmol) in 2 mL MeOH and then the reaction mixture was stirred 8 h at RT. The reaction mixture was diluted with pentane/ ether 1:1, quenched with water, washed with brine, dried over Na_2SO_4 and concentrated under reduced pressure at 20 °C. The product was carried to the next step without further purification.

R_f 0.76 (20% EtOAc/Hexane); **^{1}H NMR** (500 MHz, Chloroform-*d*) δ 7.64 (1H, d, *J* = 1.2 Hz, ArH), 7.35 (1H, t, *J* = 1.7 Hz, ArH), 6.45 (1H, dd, *J* = 1.9, 0.8 Hz, ArH), 3.03 (1H, s, H^6).

Data is in accordance with the literature.[51]

1-(3-(furan-2-yl)phenethyl)-4-(furan-3-yl)-1H-1,2,3-triazole 58

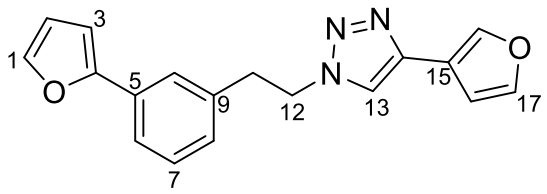

The azide **76** (115 mg, 0.54 mmol), $CuSO_4 \cdot 5H_2O$ (270 mg, 0.1 mmol) and sodium ascorbate (322 mg, 1.6 mmol) were added to the solution of alkyne **83** in water/ *tert*-butanol (1:1) and then stirred for 4 h at RT. The reaction was quenched with water and then filtered. The organics were extracted with DCM, dried over Na_2SO_4, and concentrated under reduced pressure. Purification by column chromatography (Solvent 30% EtOAc/Hexane) afforded **55** (60 mg, 38 %) as a white solid.

R_f 0.32 (30% EtOAc/Hexane); **Mp.** 101 °C; **IR**(ATR) 3109(C-H), 1444(C=C), 1049(C-O) cm^{-1}; **^{1}H NMR** (500 MHz, Chloroform-*d*) δ 7.81 (1H, dd, *J* = 1.6, 0.8 Hz, ArH), 7.56 (1H, dt, *J* = 7.8, 1.4 Hz, ArH), 7.47 – 7.45 (3H, m, ArH), 7.34 (1H, s, H^{13}), 7.31 (1H, t, *J* = 7.7 Hz, ArH), 7.00 (1H, d, *J* = 7.6 Hz, ArH), 6.67 (1H, dd, *J* = 1.8, 0.9 Hz, ArH), 6.63 (1H, dd, *J* = 3.3, 0.8 Hz, ArH), 6.47 (1H, dd, *J* = 3.4, 1.8 Hz, ArH), 4.65 (2H, t, *J* = 7.3 Hz, H^{12}), 3.27 (2H, t, *J* = 7.3 Hz, H^{11}); **^{13}C NMR** (126 MHz, $CDCl_3$) δ 153.58(C(quat), ArC), 143.61 (CH, ArC), 142.38 (CH, ArC), 140.59(C(quat), C^{14}), 139.49 (CH, ArC), 137.63(C(quat), ArC), 131.55(C(quat), ArC), 129.35 (CH, ArC), 127.82 (CH, ArC), 124.09 (CH, ArC), 122.76 (CH, ArC), 119.98(CH, C^{13}), 116.76(C(quat), ArC), 111.87 (CH, ArC), 109.01 (CH, ArC), 105.53 (CH, ArC), 51.73(CH_2, C^{12}), 36.99(CH_2, C^{11}); **HRMS** (ESI^+) Calc. for $C_{18}H_{15}N_3O_2$ [$M+H^+$] 306.1237, found 306.1231.

References

1 D. Molyneux, *Community Eye Heal.*, **2013**, 26, 21.

2 D. Legros, G. Ollivier, M. Gastellu-Etchegorry, C. Paquet, C. Burri, J. Jannin and P. Büscher, *Lancet Infect. Dis.*, **2002**, 2, 437–440.

3 P. E. Cockram and T. K. Smith, *J. Nat. Prod.*, **2018**, 81, 2138–2154.

4 Millennium Development Goals (MDGs), https://www.who.int/news-room/fact-sheets/detail/millennium-development-goals-(mdgs), (accessed 5 January 2021).

5 N. Feasey, M. Wansbrough-Jones, D. C. W. Mabey and A. W. Solomon, *Br. Med. Bull.*, **2010**, 93, 179–200.

6 N. Feasey, M. Wansbrough-Jones, D. C. W. Mabey and A. W. Solomon, *Br. Med. Bull.*, **2010**, 93, 179–200.

7 P. G. E. Kennedy, *J. Clin. Invest.*, **2004**, 113, 496–504.

8 CDC - DPDx - Trypanosomiasis, African, https://www.cdc.gov/dpdx/trypanosomiasisafrican/index.html, (accessed 4 August 2021).

9 WHO | Investing to overcome the global impact of neglected tropical diseases, https://www.who.int/neglected_diseases/9789241564861/en/, (accessed 6 July 2020).

10 D. Steverding, *Parasit. Vectors*, **2010**, 3, 15.

11 Chagas disease (also known as American trypanosomiasis), https://www.who.int/news-room/fact-sheets/detail/chagas-disease-(american-trypanosomiasis), (accessed 11 January 2021).

12 A. Rassi, A. Rassi and J. A. Marin-Neto, *Lancet*, **2010**, 375, 1388–1402.

13 P. T. Cantey, S. L. Stramer, R. L. Townsend, H. Kamel, K. Ofafa, C. W. Todd, M. Currier, S. Hand, W. Varnado, E. Dotson, C. Hall, P. L. Jett and S. P. Montgomery, *Transfusion*, **2012**, 52, 1922–1930.

14 S. Burza, S. L. Croft and M. Boelaert, *Lancet*, **2018**, 392, 951–970.

15 Leishmaniasis, https://www.who.int/news-room/fact-sheets/detail/leishmaniasis, (accessed 14 July 2020).

16 F. Chappuis, S. Sundar, A. Hailu, H. Ghalib, S. Rijal, R. W. Peeling, J. Alvar and M. Boelaert, *Nat. Rev. Microbiol.*, **2007**, 5, 873–882.

17 P. G. E. Kennedy, *Lancet Neurol.*, **2013**, 12, 186–194.

18 O. Yun, G. Priotto, J. Tong, L. Flevaud and F. Chappuis, *PLoS Negl. Trop. Dis.*, **2010**, 4, e720.

19 E. D. Deeks, *Drugs*, **2019**, 79, 215–220.

20 Drugs@FDA: FDA-Approved Drugs, https://www.accessdata.fda.gov/scripts/cder/daf/index.cfm?event=overview.process&ApplNo=214429, (accessed 4 August 2021).

21 J. A. Pérez-Molina and I. Molina, *Lancet*, **2018**, 391, 82–94.

22 J. Bermudez, C. Davies, A. Simonazzi, J. Pablo Real and S. Palma, *Acta Trop.*, **2016**, 156, 1–16.

23 J. H. No, *Acta Trop.*, **2016**, 155, 113–123.
24 D. C. Swinney and J. Anthony, *Nat. Rev. Drug Discov.*, **2011**, 10, 507–519.
25 I. H. Gilbert, *J. Med. Chem.*, **2013**, 56, 7719–7726.
26 P. E. Cockram and T. K. Smith, *J. Nat. Prod*., **2018**, 81, 2138-2154.
27 L. Katz and R. H. Baltz, *J. Ind. Microbiol. Biotechnol.*, **2016**, 43, 155–176.
28 R. Daghrir and P. Drogui, *Environ. Chem. Lett.*, **2013**, 11, 209–227.
29 A. González-Coloma, A. Guadaño, C. De Inés, R. Martínez-Díaz and D. Cortes, *Zeitschrift fur Naturforsch. - Sect. C J. Biosci.*, **2002**, 57, 1028–1034.
30 D. Fall, R. A. Duval, C. Gleye, A. Laurens and R. Hocquemiller, *J. Nat. Prod.*, **2004**, 67, 1041–1043.
31 G. J. Florence, J. C. Morris, R. G. Murray, R. R. Vanga, J. D. Osler and T. K. Smith, *Chem. - A Eur. J.*, **2013**, 19, 8309–8320.
32 A. Bermejo, B. Figadère, M. C. Zafra-Polo, I. Barrachina, E. Estornell and D. Cortes, *Nat. Prod. Rep.*, **2005**, 22, 269–303.
33 G. J. Florence, J. C. Morris, R. G. Murray, J. D. Osler, V. R. Reddy and T. K. Smith, *Org. Lett.*, **2011**, 13, 514–517.
34 L. B. Tulloch, S. K. Menzies, A. L. Fraser, E. R. Gould, E. F. King, M. K. Zacharova, G. J. Florence and T. K. Smith, , DOI:10.1371/journal.pntd.0005886.
35 G. J. Florence, A. L. Fraser, E. R. Gould, E. F. B. King, S. K. Menzies, J. C. Morris, L. B. Tulloch and T. K. Smith, *ChemMedChem*, **2014**, 9, 2548–2556.
36 A. L. Fraser, S. K. Menzies, E. F. B. King, L. B. Tulloch, E. R. Gould, M. K. Zacharova, T. K. Smith and G. J. Florence, *ACS Infect. Dis.*, **2018**, 4, 560–567.
37 K. K. Chaudhary and N. Mishra, *A Rev. Mol. Docking Nov. Tool Drug Discov. JSM Chem*, **2016**, 4, 1029.
38 A. L. Fraser, Target Elucidation of Novel Trypanosomatid Inhibitiors (PhD thesis), University of St Andrews, **2017**.
39 M. K. Zacharova, Design and Synthesis of Novel Natural Product Inspired Trypansomatid Inhibitors (PhD thesis), University of St Andrews, **2018**.
40 E. R. Gould et al (unpublished)
41 L.Liang and D.Astruc, *Coord. Chem. Rev*., **2011**, 255, 2933-2945.
42 D. Blakemore, *RSC Drug Discov. Ser.*, **2015**, 1–69.
43 D. C. Batesky, M. J. Goldfogel and D. J. Weix, *J. Org. Chem.*, **2017**, 82, 9931–9936.
44 R. Wei, L. Ge, H. Bao, S. Liao and Y. Li, *Synthesis (Stuttg).*, **2019**, 51, 4645–4649.
45 Z. Pei, C. Chen, J. Chen, J. dela Cruz-Chuh, R. Delarosa, Y. Deng, A. Fourie-O'Donohue, I. Figueroa, J. Guo, W. Jin, S. C. Khojasteh, K. R. Kozak, B. Latifi, J. Lee, G. Li, E. Lin, L. Liu, J. Lu, S. Martin, C. Ng, T. Nguyen, R. Ohri, G. L. Phillips, T. H. Pillow, R. K. Rowntree, N. J. Stagg, D. Stokoe, S. Ulufatu, V. A. Verma, J. Wai, J. Wang, K. Xu, Z. Xu, H. Yao, S.-F. Yu, D. Zhang and P. S. Dragovich, *Mol. Pharm.*, **2018**, 15, 3979–3996.
46 A. Urbano, A. M. del Hoyo, A. Martínez-Carrión and M. C. Carreño, *Org. Lett.*, **2019**, 21, 4623–4627.
47 A. P. Degnan, D. Maxwell, A. Balakrishnan, J. M. Brown, A. Easton, M. Gulianello, U. Hanumegowda, M. Hill-Drzewi, R. Miller, K. S. Santone, A. Senapati, E. E. Shields, D. V. Sivarao, R. Westphal, V. J. Whiterock, X. Zhuo, J. J. Bronson and J. E. Macor, *Bioorg. Med. Chem. Lett.*, **2016**, 26, 5871–5876.

48 J. M. Richter, D. L. Cheney, J. A. Bates, A. Wei, J. M. Luettgen, A. R. Rendina, T. M. Harper, R. Narayanan, P. C. Wong, D. Seiffert, R. R. Wexler and E. S. Priestley, *ACS Med. Chem. Lett.*, **2017**, 8, 67–72.

49 A. Höhne, L. Yu, L. Mu, M. Reiher, U. Voigtmann, U. Klar, K. Graham, P. A. Schubiger and S. M. Ametamey, *Chem. - A Eur. J.*, **2009**, 15, 3736–3743.

50 L. Shi, Y. Liu, Q. Liu, B. Wei and G. Zhang, *Green Chem.*, **2012**, 14, 1372–1375.

51 S. Kyi, N. Wongkattiya, A. C. Warden, M. S. O'Shea, M. Deighton, I. MacReadie and F. H. M. Graichen, *Bioorg. Med. Chem. Lett.*, **2010**, 20, 4555–4557.

Appendixes

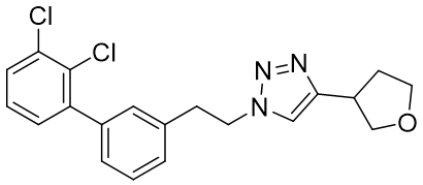

55

^{1}H NMR (500 MHz, $CDCl_3$)

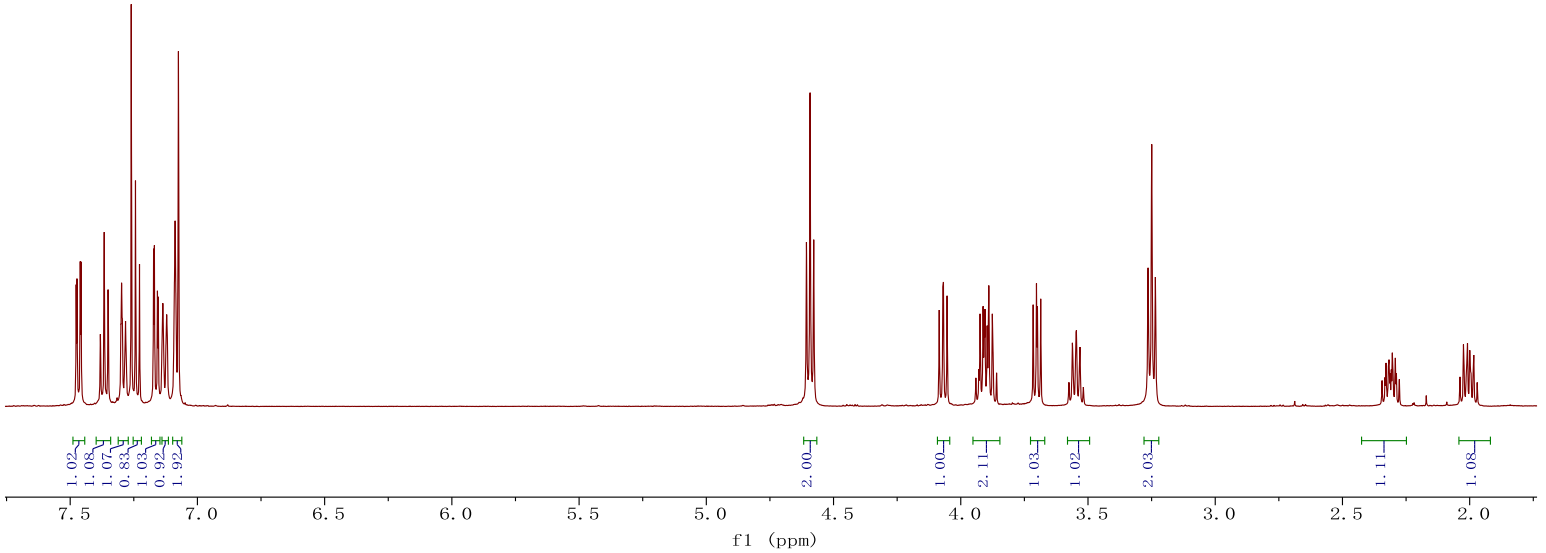

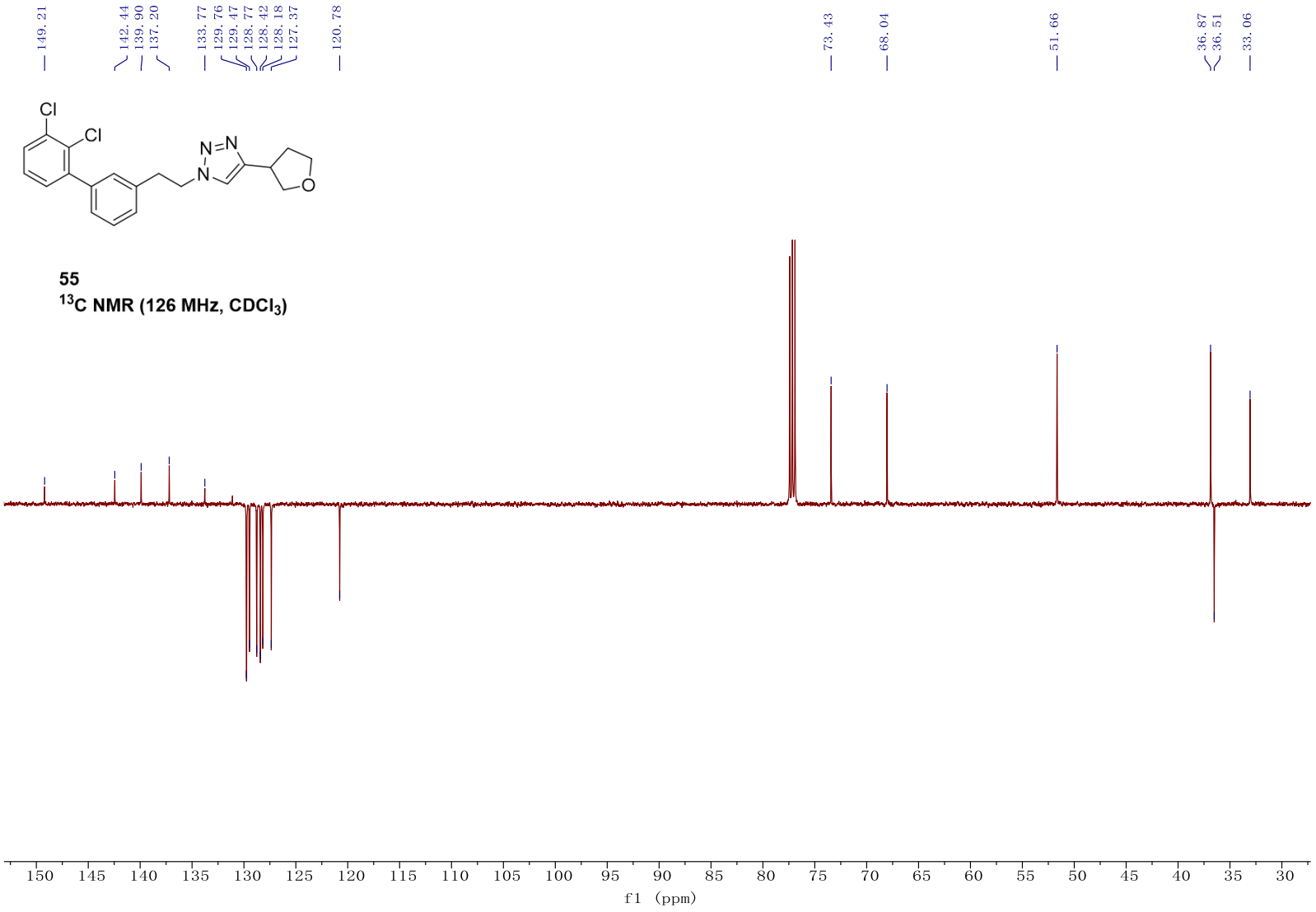
149.21
142.44
139.90
137.20
133.77
129.76
129.47
128.77
128.42
128.18
127.37
120.78
73.43
68.04
51.66
36.87
36.51
33.06
Cl
Cl
N
N
O
55
13C NMR (126 MHz, CDCl3)
150 145 140 135 130 125 120 115 110 105 100 95 90 85 80 75 70 65 60 55 50 45 40 35 30
f1 (ppm)

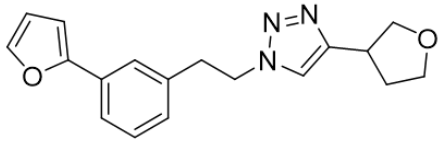

56

^{1}H NMR (500 MHz, $CDCl_3$)

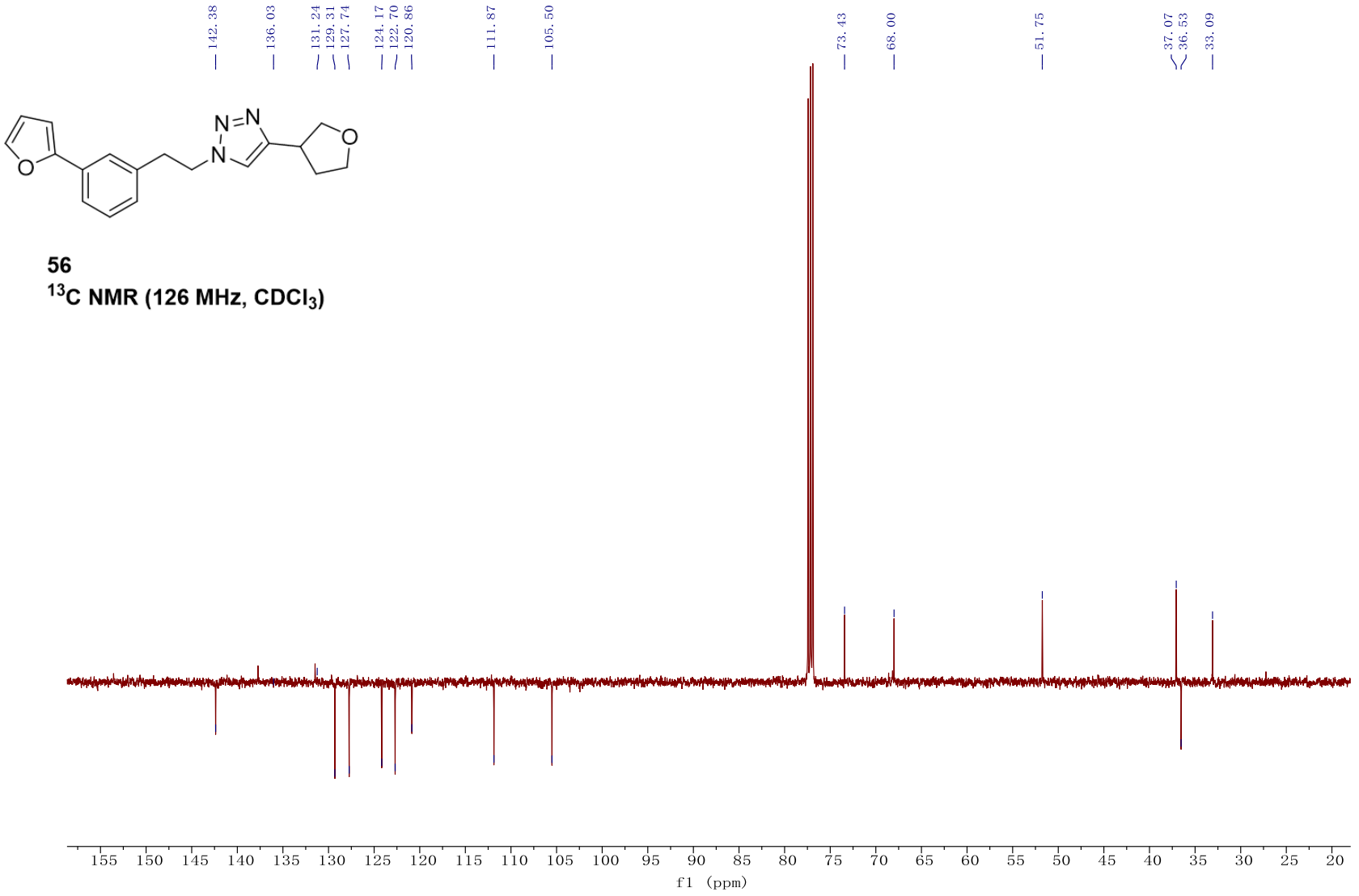

56

^{13}C NMR (126 MHz, $CDCl_3$)

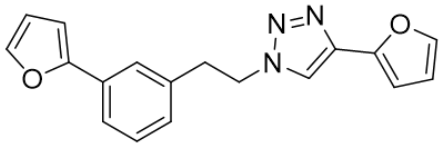

57

^{1}H NMR (500 MHz, $CDCl_3$)

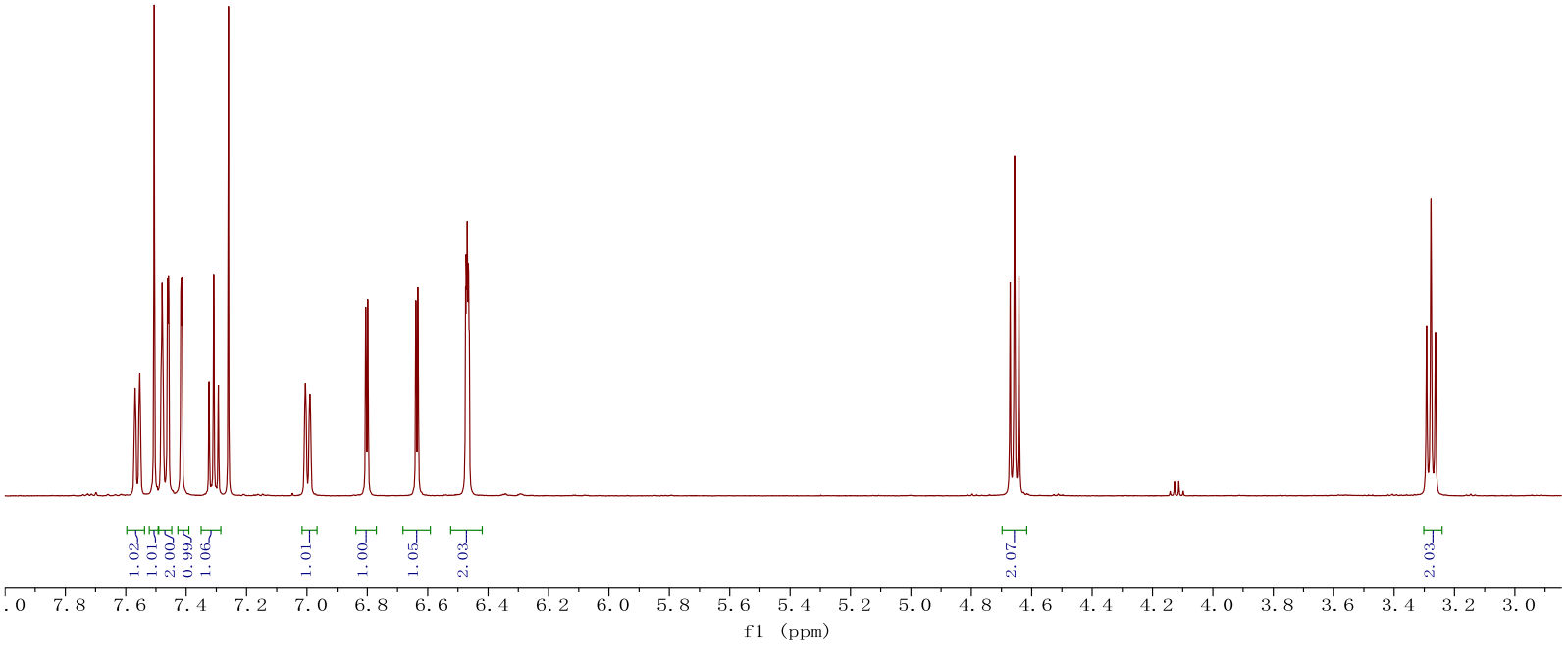

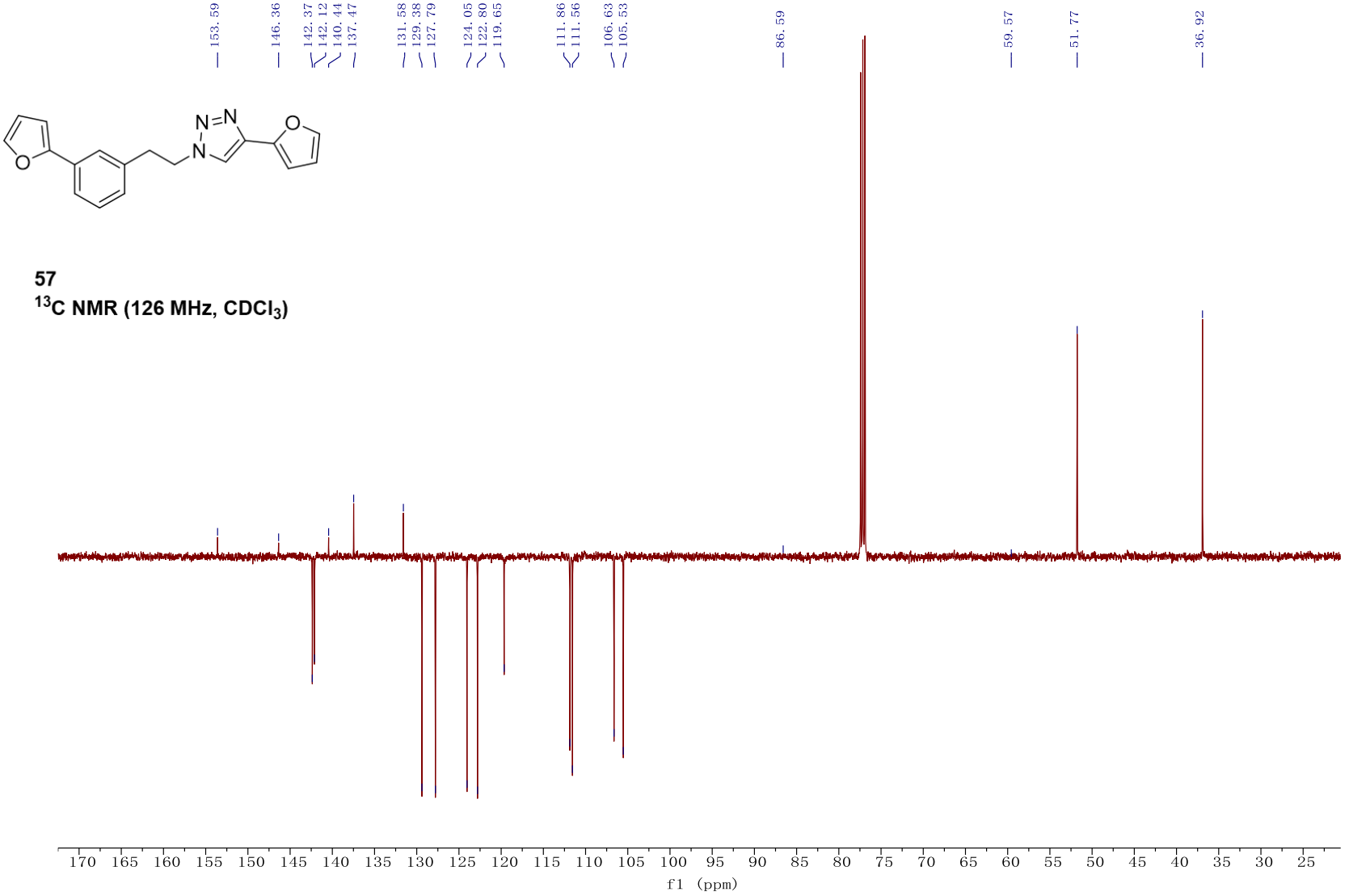
153.59
146.36
142.37
142.12
140.44
137.47
131.58
129.38
127.79
124.05
122.80
119.65
111.86
111.56
106.63
105.53
86.59
59.57
51.77
36.92
N=N
N
O
O
57
13C NMR (126 MHz, CDCl3)
170 165 160 155 150 145 140 135 130 125 120 115 110 105 100 95 90 85 80 75 70 65 60 55 50 45 40 35 30 25
f1 (ppm)

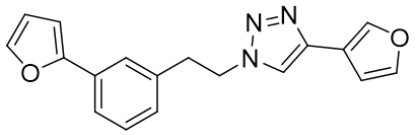

58

^{1}H NMR (500 MHz, $CDCl_3$)

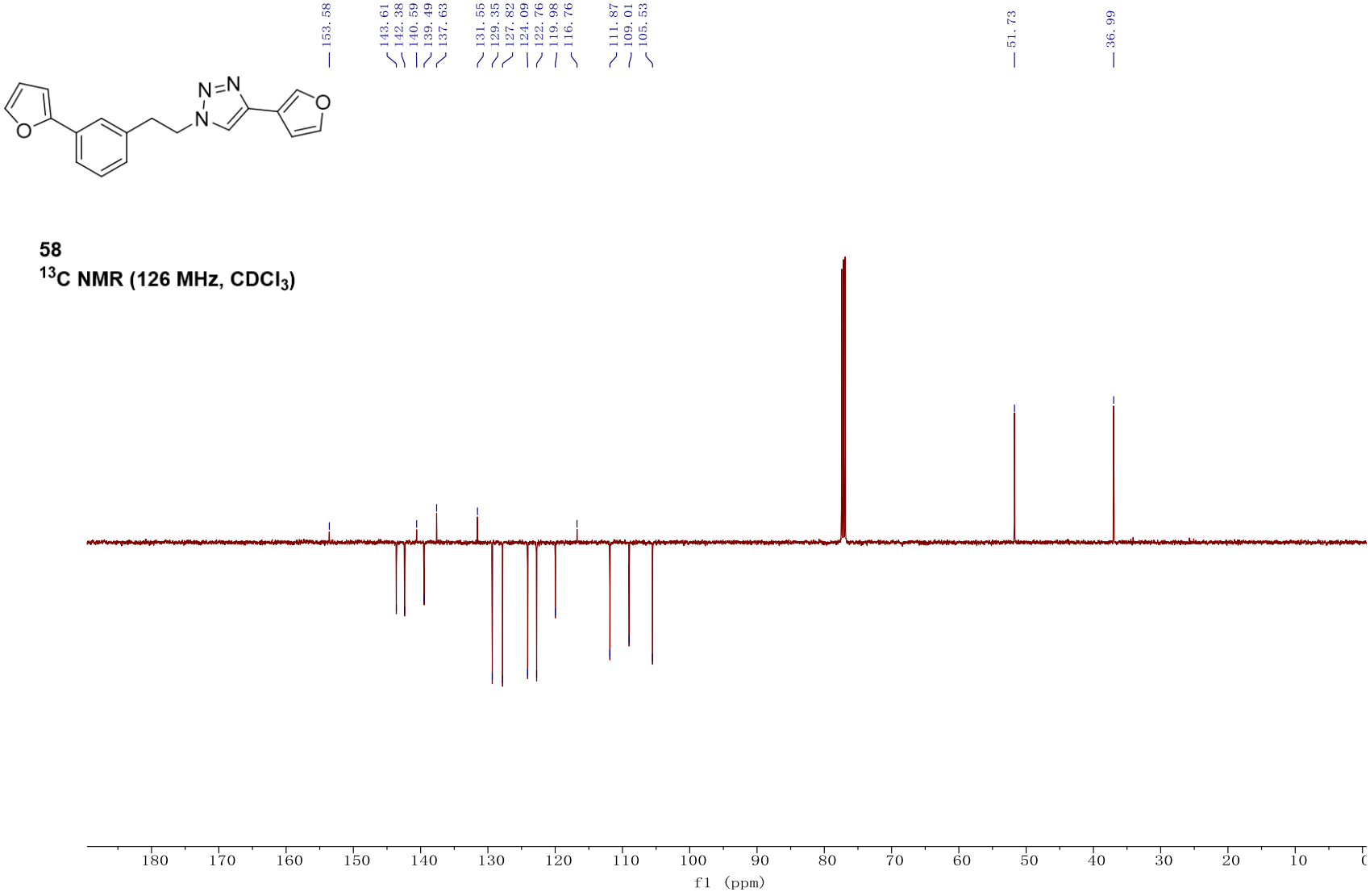
153.58
143.61
142.38
140.59
139.49
137.63
131.55
129.35
127.82
124.09
122.76
119.98
116.76
111.87
109.01
105.53
51.73
36.99
N
N
O
O
58
13C NMR (126 MHz, CDCl3)
180
170
160
150
140
130
120
110
100
90
80
70
60
50
40
30
20
10
f1 (ppm)